

AD-A150 249

SURVEY OF NONDESTRUCTIVE METHODS FOR EVALUATING
DERAILED TANK CARS(U) IDAHO NATIONAL ENGINEERING LAB
IDAHO FALLS MATERIALS SCIENCE DIV L S BELLER ET AL

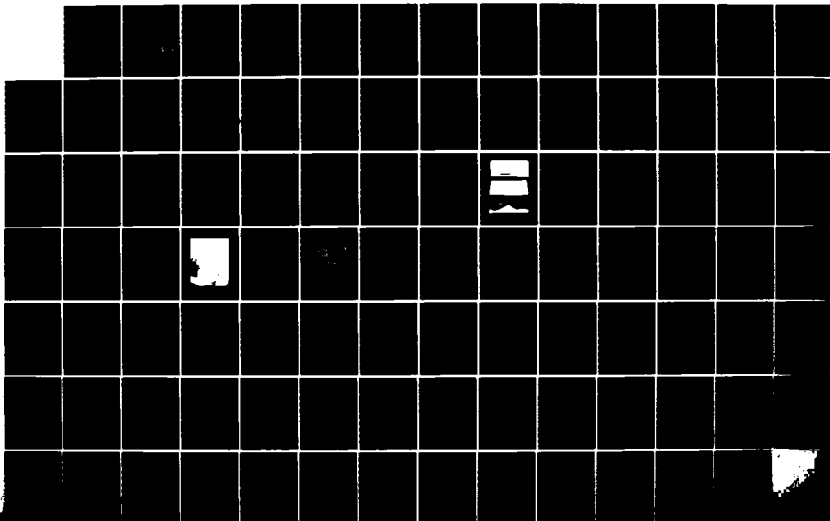
1/1

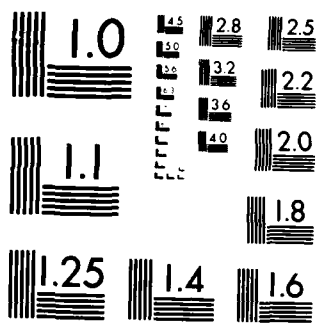
UNCLASSIFIED

NOV 84 BRL-CR-539

F/G 13/6

NL





MICROCOPY RESOLUTION TEST CHART
NATIONAL BUREAU OF STANDARDS 1963-A

12

AD-A150 249

AD -

B
R
L

CONTRACT REPORT BRL-CR-539

**SURVEY OF NONDESTRUCTIVE METHODS
FOR EVALUATING DERAILED TANK CARS**

Prepared by

Materials Science Division
Idaho National Engineering Laboratory
Idaho Falls, Idaho 83415

November 1984

DTIC FILE COPY

DTIC
ELECTE
JAN 31 1985
S B

APPROVED FOR PUBLIC RELEASE; DISTRIBUTION UNLIMITED.

**US ARMY BALLISTIC RESEARCH LABORATORY
ABERDEEN PROVING GROUND, MARYLAND**

85 01 14 011

7
Destroy this report when it is no longer needed.
Do not return it to the originator.

Additional copies of this report may be obtained
from the National Technical Information Service,
U. S. Department of Commerce, Springfield, Virginia
22161.

The findings in this report are not to be construed as an official
Department of the Army position, unless so designated by other
authorized documents.

The use of trade names or manufacturers' names in this report
does not constitute indorsement of any commercial product.

UNCLASSIFIED

SECURITY CLASSIFICATION OF THIS PAGE (When Data Entered)

REPORT DOCUMENTATION PAGE		READ INSTRUCTIONS BEFORE COMPLETING FORM
1. REPORT NUMBER CONTRACT REPORT BRL-CR-539	2. GOVT ACCESSION NO. AD-A150 249	3. RECIPIENT'S CATALOG NUMBER FRA/ORD-84/11
4. TITLE (and Subtitle) SURVEY OF NONDESTRUCTIVE METHODS FOR EVALUATING DERAILED TANK CARS		5. TYPE OF REPORT & PERIOD COVERED FINAL February 83 to October 83
7. AUTHOR(s) L.S. Beller, J.D. Mudlin, W.G. Reuter, M.A. Tupper		5. PERFORMING ORG. REPORT NUMBER
9. PERFORMING ORGANIZATION NAME AND ADDRESS Materials Science Division Idaho National Engineering Laboratory Idaho Falls, ID 83415		8. CONTRACT OR GRANT NUMBER(s) A.N. DTR55-82-X-00275
11. CONTROLLING OFFICE NAME AND ADDRESS US Army Ballistic Research Laboratory ATTN: AMXBR-OD-ST Aberdeen Proving Ground, MD 21005-5066		10. PROGRAM ELEMENT, PROJECT, TASK AREA & WORK UNIT NUMBERS
14. MONITORING AGENCY NAME & ADDRESS (if different from Controlling Office)		12. REPORT DATE NOVEMBER 1984
		13. NUMBER OF PAGES 92
		15. SECURITY CLASS. (of this report) UNCLASSIFIED
		15a. DECLASSIFICATION/DOWNGRADING SCHEDULE
16. DISTRIBUTION STATEMENT (of this Report) Approved for public release, distribution unlimited.		
17. DISTRIBUTION STATEMENT (of the abstract entered in Block 20, if different from Report)		
18. SUPPLEMENTARY NOTES This study was funded by the Federal Railroad Administration of the Department of Transportation		
19. KEY WORDS (Continue on reverse side if necessary and identify by block number) Railroad Tank Cars Safety Nondestructive Evaluation Fracture Mechanics		
20. ABSTRACT (Continue on reverse side if necessary and identify by block number) This study concerns the development of procedures for assessing a derailed tank car loaded with hazardous materials prior to movement or the unloading of the tank car's lading. The technology needed to predict the level of safety consists of the following: (1) A system(s) to determine the probability of rupture from a remote location for the purpose of deciding if it is safe for personnel to approach the tank car; (2) Assuming the tank car has been safely approached, then a contact system(s) is required to evaluate the damaged		

DD FORM 1 JAN 73 1473

EDITION OF 7 NOV 83 IS OBSOLETE

UNCLASSIFIED

SECURITY CLASSIFICATION OF THIS PAGE (When Data Entered)

UNCLASSIFIED

SECURITY CLASSIFICATION OF THIS PAGE(When Data Entered)

region for the purpose of determining the probability of rupture in the event the tank car is moved or unloaded, and (3) A real-time monitoring system(s) is required to detect a change in the condition of the tank car as it is being moved or unloaded and provide immediate warning to the wreck-clearing crew of impending failure or rupture. The contents of this report are the results of a preliminary evaluation of the technology required, details of technical findings, and identification of areas of needed research.

Accession For	
NTIS GRA&I	<input checked="checked" type="checkbox"/>
DTIC TAB	<input type="checkbox"/>
Unannounced	<input type="checkbox"/>
Justification	
By	
Distribution/	
Availability Codes	
Dist	Avail and/or Special
A-1	



UNCLASSIFIED

SECURITY CLASSIFICATION OF THIS PAGE(When Data Entered)

EXECUTIVE SUMMARY

EG&G Idaho, Inc., prime operating contractor of the Idaho National Engineering Laboratory, was requested by the Ballistic Research Laboratory (BRL), Aberdeen Proving Ground, Maryland to become involved in a BRL effort to resolve problems associated with the evaluation of derailed tank cars carrying hazardous materials. This is part of a broad research program BRL is performing for the Federal Railroad Administration (FRA) in Railroad Safety Research. Thus, the funding for this work was provided by the FRA. The key issue is to develop procedures for assessing the level of safety for the benefit of those involved in moving and/or unloading the damaged tank car.

The technology needed to predict the level of safety consists of the following systems:

1. A system(s) to determine the probability of rupture from a remote location for the purpose of deciding if it is safe for personnel to approach the tank car.
2. Assuming the tank car has been safely approached, then a contact system(s) is required to evaluate the damaged region for the purpose of determining the probability of rupture in the event the tank car is moved or unloaded.
3. Finally, a real-time monitoring system(s) is required to detect a change in the condition of the tank car as it is being moved or unloaded and provide immediate warning to the wreck-clearing crew of impending failure or rupture.

EG&G Idaho was requested by BRL to perform a preliminary evaluation of the technology required for the above items. This document provides details of the findings and identifies areas of needed research. These are summarized as follows:

1. Remote Sensing Capabilities

Remote sensing equipment may consist of, but is not limited to, an infrared system for detecting leaks in the tank car and moire and/or laser systems for measuring the extent of indentation of the damaged area. The extent of the indentation can be related to wall thinning, which in turn can indicate the change in fracture toughness and the stress associated with the deformation and allow estimates of the amount and seriousness of wall cracking.

This preliminary analysis has established that a correlation does exist between wall thinning and the amount of cracking. Also, it has been shown that wall thinning correlates with the reduction of fracture toughness. However, the data sample is limited and in order to gain a high confidence and to quantify these observations, it is necessary to analyze more than the few specimens which have been studied thus far. For the purpose of verifying these conclusions, a "typical tank car" damaged in a real accident should be studied and the result compared with the sample data.

2. Contact Sensing Capabilities

The preliminary evaluation of ten indented plates made of a typical tank car steel shows that ultrasonic techniques constitute a quick and accurate method for measuring wall thickness, locating and characterizing cracks, and estimating metallurgical changes. The accuracy of the ultrasonic techniques for detecting cracks which have penetrated the surface of the steel plate has been verified by using dye penetrant. There are other NDE techniques which may be of benefit in specific situations, but ultrasonic techniques are superior in the general case. One difficult situation is that the tank car may have a thermal coating over the outer shell and, in that case, the coating would have to be removed in order to use ultrasonic

techniques. However, while the coating is being removed, the tank car can be monitored for crack growth by using acoustic emission techniques.

3. Real-Time Monitoring Capabilities

As the tank car is being moved or unloaded, its condition should be monitored with the acoustic emission devices mentioned above. In that case, available techniques need to be modified to permit the separation of acoustic emissions from other noise generated as the tank car is being moved. Experience from previous studies by EG&G Idaho has shown that the detection of crack growth in materials similar to those used in tank cars is feasible.

In addition to the detection and characterization of flaws in the tank car, it is necessary to determine the critical flaw size that would cause failure in the undamaged tank car material and the critical stress for failure in the damaged tank car. A literature search of ASTM A515-70 type steel revealed that there is insufficient information to develop a data base. This prevented a statistical analysis to determine the probability of overestimating the plane strain fracture toughness (K_{Ic}). For the damaged tank car, where the wall thickness had been reduced 25%, estimates of K_{Ic} of 40% and 30% of the K_{Ic} estimate for undamaged steel (100% wall thickness) were used in the fracture mechanics analysis (LEFM concepts) to predict the conditions for failure.

Due to time and materials limitations, it was not possible to perform valid K_{Ic} measurements, and estimates were made using the true stress/true strain curve generated from tensile tests of A515-70 steel. Nor was it possible, for the same reasons, to determine if the change in K_{Ic} is due to an increase in the nil ductility transition temperature (NDTT) or to a decrease in the upper shelf value.

The calculations and analyses performed indicate that LEFM techniques are useful for predicting failure conditions and identify the areas where additional work is needed. Based on LEFM analysis (calculation of critical

flaw size/critical applied stress values based on K_{Ic}), the parameters necessary to predict the safety of moving a damaged tank car are identified and recommendations made to increase accuracy and reduce the conservatism of these predictions.

Ultimately, it will be necessary to relate the real conditions prevailing in an accident to the basic data. Thus, it will be necessary to determine the level of stresses the tank car will experience, relate this information to the data base, and then predict the safety level. A valuable tool would be a stress analysis program which would compute the stress levels throughout the tank car, given the loads expected when the tank car is moved. This would allow studies which could provide guidelines on how to move the tank car with the minimum amount of stress in weakened regions.

To verify the models generated in these studies, experiments need to be conducted on model tank cars instrumented with strain gages, accelerometers, acoustic emission sensors, and perhaps other NDE devices. Once the procedures are fully developed and verified for model tank cars, then a full size tank car test for verification may be justified.

CONTENTS

	Page Number
LIST OF FIGURES	9
LIST OF TABLES	11
1. INTRODUCTION	13
2. SURVEY OF NONDESTRUCTIVE EVALUATION TECHNIQUES	18
2.1 Information Obtainable by NDE	18
2.1.1 Leaks	19
2.1.2 Deformation Caused by the Accident	19
2.1.3 Cracks, Tears, and Ruptures	20
2.1.4 Surfaces and Surface Conditions	20
2.1.5 Subsurface Conditions	20
2.2 NDE Techniques	20
2.2.1 Visual Inspection	21
2.2.2 Infrared Techniques	21
2.2.3 Acoustic Emission	22
2.2.4 Magnetic Particle NDE	23
2.2.5 Eddy Current NDE	24
2.2.6 Liquid Penetrant NDE	25
2.2.7 Other Surface Inspection Techniques	25
2.2.8 Radiography	27
2.2.9 Ultrasonics	29
2.2.10 Other NDE Techniques	31
2.3 NDE Survey Conclusions	32
3. NDE EVALUATION OF FLAT PLATE SPECIMENS	34
4. FRACTURE MECHANICS	47
4.1 Estimates of Fracture Toughness	48
4.1.1 Calculations of Fracture Conditions	50
4.1.2 Critical Flaw Sizes for Undamaged Tanks	54
4.1.3 Failure Conditions for a Damaged Tank Car	55
4.2 Discussion	55
4.2.1 Undamaged Tank Cars	58
4.2.2 Damaged Tank Car	58
4.2.3 General Discussion	52

5. SUMMARY, CONCLUSIONS, AND RECOMMENDATIONS	64
5.1 Visual Observations	65
5.2 Ultrasonic Examination	65
5.3 Fracture Mechanics	66
6. REFERENCES	68
APPENDIX A - PLATE THINNING DATA.....	69
LIST OF SYMBOLS.....	89
DISTRIBUTION LIST	91

LIST OF FIGURES

	Page Number
1. Three Views of a Flat Plate Specimen Showing General Dent Shape	35
2. Dial Micrometer Measurements of Dent Depth	37
3. Typical Plot of Thickness Versus Position Obtained by Use of Ultra- sonic Thickness Gauge (Plate No. DH-26-04-83-16-160)	37
4. Thickness Plot Showing Severe Thinning of a Plate Specimen	38
5. Thickness Plot for Plate Specimen Which Was Not Deformed Enough to Possess Severe Thinning	38
6. Typical Map of Surface Cracks on the Convex (Bottom) Side of a Flat Plate Specimen	39
7. Area of Surface Cracking as a Function of Percent Reduction in Thickness	42
8. Area of Surface Cracking as a Function of Dent Depth	42
9. Number of Cracks as a Function of Dent Depth	43
10. Total Length of Cracks as a Function of Dent Depth	43
11. Ultrasonic Examination of Flat Plate Specimen	44
12. Contour Plots Generated by the Ultrasonic Imaging System of Flaws in Metal	46
13. Thickness Measurements (mm) and Location of Test Specimens Removed From Plate DH-26-04-83-16-160	51
14. Thickness Measurements (mm) and Location of Test Specimens Removed From Plate DH-26-04-83-22-160	52
15. Correlation Between Applied Stress Intensity Factor and Crack Depth for Two Extremes in Aspect Ratio for the Undamaged Tank Car	56
16. Correlation Between Applied Stress and Crack Depth for Three Values of K_{Ic} with $a/2c = 0.1$	57
17. Correlation Between Applied Stress and Crack Depth for Three Values of K_{Ic} with $a/2c = 0.5$	61

LIST OF TABLES

	Page Number
1. CORRELATION OF MEASURES OF DEGREE OF SURFACE CRACKING AND DEFORMATION	40
2. CHEMISTRY AND MECHANICAL PROPERTIES OF ASTM A-515 GRADE 70 STEEL	49
3. MECHANICAL PROPERTIES FOR PLATES 16 AND 22	53
4. CALCULATED CONDITIONS FOR FRACTURE	59

1. INTRODUCTION

EG&G Idaho, Inc., the prime operating contractor of the Idaho National Engineering Laboratory (INEL), was commissioned by the Ballistic Research Laboratory (BRL) to assist in an effort to resolve problems associated with the evaluation of derailed tank cars carrying hazardous materials. The BRL was under contract with the Federal Railroad Administration (FRA), Department of Transportation (DOT), to conduct a study dealing with the safety aspects of clearing wrecked tank cars loaded with hazardous materials under pressure. The key issue is to develop procedures which will enable personnel to accurately predict the level of safety for those involved in moving and/or unloading the damaged tank car. INEL was requested by BRL to become involved due to its extensive experience and knowledge in the field of nondestructive evaluation (NDE).

The historical information which supports the decision to do this work includes the fact that 24 fatalities and 118 injuries have been sustained in recent years due to tank car ruptures during wreck-clearing operations. The worst occurred following a 23-car derailment at Waverly, Tennessee on February 24, 1978.¹ In that incident, a damaged tank car containing liquid petroleum gas (LPG) ruptured two days after a derailment, during preparations for having its lading transferred. The lading was released and the ensuing fire killed 16 persons and injured 43 others. Another incident occurred on April 18, 1979 at Crestview, Florida where several wreck-clearing personnel were exposed to anhydrous ammonia from a tank car which unexpectedly ruptured.² These incidents show that wreck-clearing crews, emergency response teams, and the public are in danger even after the initial hazards in a derailment involving hazardous materials have been neutralized.

¹"Railroad Accident Report-Derailment of Louisville and Nashville Railroad Company's Train No. 584 and Subsequent Rupture of Tank Car Containing Liquid Petroleum Gas, Waverly, Tennessee, February 22, 1978," NTSB-RAR-79-1, U.S. National Transportation Safety Board, February 1979.

²"Railroad Accident Report-Louisville and Nashville Railroad Company Freight Train Derailment and Puncture of Hazardous Materials Tank Cars, Crestview, Florida, April 18, 1979," NTSB-RAR-79-11, U.S. National Transportation Safety Board, September 1979.

The historical evidence caused the National Transportation Safety Board to initiate a special investigation to identify the hazards caused by the reduction of the ability of damaged cars to contain their lading; to determine the ability of experts to estimate this reduced capability; and to examine the feasibility of developing practical guidelines to help determine how a damaged hazardous materials tank car should be handled.³ This study used a tank car which had sustained a large dent in derailment, but had not ruptured as it was returned upright back on the track and the hazardous material (vinyl chloride) unloaded. The tank car was examined by a group of experts using dye penetrant and portable magaflex NDE equipment, both on the inside and the outside of the tank car. No cracks were found by this inspection. The experts then predicted that the dent would begin to deflect outward at a pressure estimated to range from 75 to 290 psi with no predictions that a rupture would occur below the design-tested pressure level of 340 psi. However, when the tank car was hydrostatically tested, the dent began to deflect at 40 psi and the tank car ruptured at 205 psi. The most important conclusion resulting from the study was that there is currently no accurate method for estimating the residual strength of a damaged railroad tank car.

There are actually three situations where NDE techniques are applicable in dealing with tank cars: manufacturing, inservice inspection, and after sustaining damage. During manufacturing it is relatively easy to use NDE since the procedures can be systematized to fit the constant routine of construction. A more difficult situation is routine inspection of tank cars during their lifetime of service. In that case, the cars are fully constructed with geometries not so amenable to systematic procedures. For example, the tank car may have a thermal coating, a jacketed insulation system, or both. However, the most difficult application is the evaluation of a damaged tank car in the field. In that case, the geometry can vary according to the size and shape of the dent and the position of the tank car. It is anticipated that the NDE procedures required will be difficult to systematize and in some cases the evaluation may have to be performed at a remote location from the tank car. The effort reported here was concentrated on the third situation since it is

³"SPECIAL INVESTIGATION REPORT — Tank Car Structural Integrity After Derailment," NTSB-SIR-80-1, U.S. National Transportation Board, October 16, 1980.

believed that the solution for the two previous situations will occur automatically from the research effort on the third.

There are four steps in the assessment problem of a derailed tank car: remote evaluation, close-up evaluation, moving/unloading, and suitability for further service. Since the tank car will be loaded with a hazardous material, it will be necessary to assess from a distance the safety of approaching it to perform a close-up evaluation. One of the first problems is to determine if the car is leaking and, if it is, based on a knowledge of the contents of the car, determine the appropriate action. If no leaks are detected, then by relating the dent size and depth to possible flaws (such as a crack), it must be determined if the car can be approached safely. This will be a gross evaluation of the tank car and will be based on correlation of flaw data with characteristics of the dent.

The next step is to perform a close-up evaluation of the tank car with NDE techniques which require actually touching the tank car. In this case, the flaws in and around the dent will be detected and the signatures of these flaws fed directly into a computer. The computer will compare the signatures with a memory data base and then automatically read out the type of flaws and their potential for rupture as a function of applied strain. The data base will be obtained by studying tank car steel specimens and will consist of flaw signatures, stress-failure data, and corresponding strain values. The result of this assessment will be a determination of the safety of moving or unloading the tank car. The level of care to be taken will depend on the type of hazardous material in the tank car and the estimate of the chances of a rupture.

The third step is to monitor the tank car as it is being moved or unloaded. The purpose of the monitoring system is to instantly detect crack initiation, crack growth, and tank car leakage to provide an immediate alarm to the wreck-clearing personnel to stop operations and clear the area. In the event of a rupture, a few seconds warning can be the difference in the occurrence of casualties or a safe retreat of the wreck-clearing personnel.

The final step is to evaluate the unloaded car for the purpose of repair and final assessment to determine if it meets safety requirements for continued service.

Fundamental requirements of an overall system are the following:

1. Remoteness and Quickness

Remote sensing should be used to the maximum extent possible for the safety of personnel. Due to the fact that the situation may be developing rapidly, there should be an emphasis on speed, immediacy, and timeliness of the information to be gathered.

2. Accurate Determinations

Due to the high potential for loss of lives and property, an accurate determination of the condition of the tank car is required. A significant body of basic metallurgical, stress, structural, and historical data need to be developed and made available for correlation in the field with NDE findings.

3. Portability

Techniques employing equipment or information which cannot be assembled on the accident site immediately will contribute little to the required assessment. The need for portability places a constraint on the various techniques which can be employed and requires development of an overall systematic approach.

In support of the BRL investigation, EG&G Idaho conducted a survey of NDE techniques and performed an NDE evaluation and fracture mechanics analysis of ten indented specimens of a typical tank car steel. The experimental NDE effort provided very encouraging results, in nearly every instance confirming initial hypotheses on what could be expected. The NDE's and fracture mechanics' work presented are very preliminary and represent a very small statistical base. Confirmatory measurements in other materials

are clearly needed. Extended efforts involving measurement of additional variables are also needed. Finally, it is clear that, to be useful, these efforts must be extended to a significantly greater statistical base, with many more specimens investigated in detail.

2. SURVEY OF NONDESTRUCTIVE EVALUATION TECHNIQUES

Nondestructive evaluation (NDE) is a large and rapidly developing field. The field is solidly based on what may be called the "classical" techniques such as radiography, ultrasonics, and penetrant testing. In addition, there is a growing body of very sophisticated instruments and analytical methods, based on these classical techniques, which are capable of extracting considerably more information. Further, there is a similarly growing body of NDE techniques based on physical principles that are new to the field, and which can be extremely useful in appropriate circumstances. The successful practice of NDE using any technology must include well-thought-out and methodically used procedures and protocols and must correlate the data obtained with physical, structural, and historical information.

The NDE techniques are only a portion of the overall system required for tank car damage assessment and should be considered in the framework of a system which (a) assesses the current status, safety, and structural integrity of the damaged tank car, and (b) predicts the same with the greatest possible accuracy for successive future operations. This section is a survey of NDE techniques, both classical and more recent, which may be applicable to damaged tank car assessment at various stages of the accident-recovery scenario developed in the previous section. The choice of appropriate methods depends on the conditions under which they will be used, on the observations that can be made, and the information that can be gained from them at each stage, and on background information which is or can be made available to assist in the assessment. These are discussed briefly below to assist in evaluating the NDE techniques to be considered.

2.1 Information Obtainable by NDE

Some of the measurements which can potentially be made by NDE are discussed here.

2.1.1 Leaks

A relatively large leak may be visually observable. Somewhat smaller leaks may be detected by their effects on the local temperature. Both the adiabatic expansion of a compressed gas and the heat of vaporization of a liquid/vapor phase change lower the temperature of the escaping vapor and its immediate surroundings. Thus, the detection of local cold spots is an important technique for locating leaks and remote sensing of these temperature differences can be important in the early stages of the accident-evaluation.

The importance of smaller and smaller leaks increases as personnel approach a damaged tank car. Furthermore, it is especially important to quickly detect leaks that develop during unloading operations, or as a loaded car is being moved or handled. Fortunately, the turbulence of an escaping compressed gas almost always generates a "whistle" that can be detected with appropriate instruments. The sound is usually impulsive, and depending on the circumstances, can range in pitch from sub-audible through the range of human hearing to the ultrasonic range. A sudden change in characteristics of such a whistle can indicate the onset of an unsafe condition.

2.1.2 Deformation Caused by the Accident

The deformation is, in itself, an important indicator of the tank car's status, and can point to the locations of potential structural weakness. If the degree of deformation can be reliably correlated to the mechanical properties which determine structural integrity, such as section thickness, residual strength, and fracture toughness, deformation measurement would be a very powerful tool for assessment. Since deformation can be measured remotely, this important safety information can be obtained early in the process.

There are several possible measurements of deformation for use in damage assessment. These include dent radius and depth, thinning in deformed areas, and changes in the relative positions of tank car

components. (An example of the latter would be a truck out of alignment. Depending on the design of the tank car, this could indicate severe stress and possible damage to the structural integrity at its point of attachment which may be located far from obvious denting.)

2.1.3 Cracks, Tears, and Ruptures

Cracks, tears, and ruptures range from minor surface phenomena to major openings which may or may not be leaking. Cracks can be observed by a number of techniques. The larger cracks will be located in areas of actual strength reduction, and all cracks point to areas of potential reduction in the mechanical properties which determine the car's structural integrity.

2.1.4 Surfaces and Surface Conditions

The surface conditions are primarily qualitative indicators of areas of disturbance and possible damage. Severe rusting, for example, indicates areas of possible structural weakness and potentially increased damage due to the stresses of an accident. The movement, flaking, or chipping of paint, coatings, or insulation can also indicate areas which may be damaged. On a different level, local change in the texture of a metallic surface often indicates severe metallurgical damage.

2.1.5 Subsurface Conditions

Hidden subsurface cracks, physical discontinuities, and defects of all kinds are observable by a number of NDE techniques. Some techniques are capable of detecting local changes in mechanical properties, under some conditions at least, in otherwise "solid" metal.

2.2 NDE Techniques

NDE techniques are required which can be deployed rapidly under emergency field conditions, observe the quantities discussed, and yield reliable results. It should be understood that considerable work may be

necessary beforehand to obtain the metallurgical, structural, stress, and historical information to correlate with the NDE results to give a complete and accurate assessment rapidly. The following techniques may be useful for this problem.

2.2.1 Visual Inspection

The eye of an intelligent, trained observer, properly supported, is one of the most effective NDE tools available. In areas where capabilities overlap, visual techniques generally yield results that are far superior to any other. They are especially applicable to assessment from a safe distance.

Proper support for visual inspection includes training, written procedures and checklists carefully prepared in advance, and appropriate tools. Appropriate tools may include telescopes, lighting, and comparison standards for determining alignment and deformation. Visual techniques are capable of determining the contours of major deformations and measuring their parameters remotely. It has been demonstrated, for example, that appropriate moire patterns projected optically on a surface can quickly reveal changes in contour and assist in accurate measurement of the extent and depth of denting and deformation. Laser surveying instruments can be used to measure relative deformations precisely if necessary.

Supported visual examination is most applicable to the preliminary stages of the scenario, which include assessment of large leaks, assessment of deformations of all kinds, and observations of surface conditions and areas of potential damage. Closeup observations later on can extend this general information to finer details of importance.

2.2.2 Infrared Techniques

All objects at temperatures above absolute zero emit electromagnetic radiation with amplitude and frequency spectra that depend on the

temperature and on the object's surface emissivity. At temperatures below incandescence, the emitted radiation is in the infrared and longer wavelength regions of the spectrum.

Commercially available instruments sensitive to infrared radiation are often capable of measuring temperature differences that are smaller than one degree Fahrenheit. Some are capable of forming infrared images on a television-like device with good resolution. Such images allow the operator to visualize or pinpoint areas of anomalous hot or cold. These devices, and companion instruments which measure the temperature along a line or at a spot, form the basis for infrared NDE. With appropriate procedures, techniques, and experience, infrared NDE is used regularly in many industrial settings for such purposes as evaluating insulation and determining the performance of electrical transformers. An important characteristic is its ability to make remote measurements.

Infrared NDE appears to be applicable to leak detection for damaged tank cars. The liquid/gas phase change and adiabatic expansion of gases will provide a significant degree of local cooling at the point of the leak, in the vapor cloud, in any accumulation of liquid on the ground, and in the immediate surroundings of these places. Infrared imaging should reveal the presence of all but the smallest leaks from a safely remote location.

2.2.3 Acoustic Emission

Most physical processes generate molecular or atomic motions which travel as elastic or acoustic waves. Examples of processes which generate acoustic waves are the turbulent flow of a gas or liquid, the formation of cracks and tears in metallic structures, and plastic strain of metallic structures. These processes cause sound waves at frequencies ranging from fractions of a hertz to megahertz with intensity values having a similarly large range. The discipline of acoustic emission monitoring is based on these properties.

Acoustic emission instruments and techniques have been developed for application over a substantial frequency and sensitivity range. Acoustic emission is used routinely to monitor tensile, fracture, and fatigue tests. It is possible to detect plastic deformation during tensile testing by using a sensitive system. In fracture and fatigue tests, a lower sensitivity is used to detect crack growth. Crack growth signals can be separated from interfering sources of noise coming from outside of the region of interest. In industrial applications, acoustic emission is used to monitor hydrostatic tests of pressure vessels and piping systems. A number of other applications are also routine.

The success of acoustic emission is based on the fact that acoustic waves can be detected at some distance from their origin. Arrays of transducers and electronic systems are used to measure the relative time of arrival of the wave at each transducer; then a relatively simple computer program solves the seismic equations (exactly as in earthquake detection) to identify the stress point (the "epicenter") from which the sound originated. The system rejects those sound waves which are originated outside the designated region of interest.

It appears that acoustic emission techniques may have several applications in the present problem. Once it has been determined that the damaged tank car is safe to approach, one or more acoustic emission sensors having the appropriate frequency range could be used to detect (from a distance, once the sensor has been placed in contact) crack growth and/or small leaks. Changes in emission characteristics might later be used as an early warning while personnel are working near the car. Acoustic emission techniques could be used at later stages when the damaged car is being raised or moved to pinpoint structural changes caused by a redistribution of stresses.

2.2.4 Magnetic Particle NDE

Discontinuities in magnetized ferromagnetic materials disturb the residual magnetic field, increasing its strength near the discontinuity. Very fine magnetic powders or particles, often dyed brilliant colors, are

attracted to these anomalies in the magnetic field and outline minute surface and subsurface discontinuities. The most familiar use of the technique is in testing automotive components for cracks, but much more sophisticated and sensitive equipment is employed in many industries, including aerospace and nuclear.

In applying the technique, one first magnetizes the component to be tested. The method of magnetization varies, depending on the shape and size of the component. Encircling coils and contact coils carrying large currents are used frequently. In some systems, the part being tested is itself used to carry the magnetizing current. It is important that the direction of the resulting magnetization be perpendicular to the direction of the discontinuity to be detected; often several magnetizations are required. It is important to note that changes in shape or contour of the part being tested, such as at welds or corners, also distort the magnetic field and give false indications; separating true from false indications requires a skilled operator.

The large currents required for magnetization, even though they are usually at low voltages, raise the possibility of sparks should the equipment or cable malfunction or the operator err; this is highly undesirable. The process as commonly used would require the presence of a trained operator at the damaged car. Magnetic particle NDE would be difficult to automate for remote use and does not provide a significant advantage over other surface and subsurface crack detection methods which are more amenable to the situation.

2.2.5 Eddy Current NDE

Eddy current NDE is used, like magnetic particles, to detect surface-breaking and slightly subsurface cracks and similar defects. The eddy current probe is a coil which is designed to be the primary winding of a transformer. It is held mechanically in close proximity to the surface to be evaluated. Alternating current, typically at audio frequencies, in the coil induces currents in the part being examined while the part itself becomes, in effect, a single-turn shorted secondary winding of the

transformer. As the coil passes over a defect in the part, the path taken by the induced eddy currents changes from what it had been in nearby sound metal, generally becoming longer. The changed impedance seen by the eddy currents is reflected electrically into the primary coil circuit where it is measured as a change in the phase of the excitation current. The phase changes can be calibrated in terms of crack parameters such as depth.

The technique is difficult to apply to ferromagnetic materials. In this situation, several different frequencies are usually used, either simultaneously or in sequence, and defect detection is based on functions of the differences in response between frequencies.

Eddy current NDE is sensitive to any change in impedance, not just to those changes caused by cracks. Changes in impedance can come from changes in cross section, changes in the relative geometry between part and probe, inhomogeneities in the metal, and the presence of a nearby part, such as stiffeners. The technique finds its most important uses in those inspection situations where the geometry is well defined and uniform, such as tubing and sheet metal inspection and inspection of fastener holes for radial cracking.

In general, the disadvantages of eddy current NDE outweigh its usefulness for inspecting damaged tank cars in the field.

2.2.6 Liquid Penetrant NDE

This technique is based on liquids whose surface tension and viscosity have been adjusted so that the liquid penetrates into very small and narrow openings, such as fine hairline cracks. The liquid usually is brightly colored or includes materials which fluoresce under ultraviolet light.

In use, the part to be examined is brushed to remove loose scale and dust. Then it is cleaned to remove oils and greases; vapor degreasing is the preferred method when possible, but appropriate solvents are often used. The penetrant is then applied and allowed to stand on the part long

enough for the liquid to penetrate into the cracks; five or ten minutes is typical. Excess penetrant is carefully removed from the surface and a "developer" is applied. The developer is usually a finely powdered dry solid such as chalk, which now reverses the process and draws the penetrant from the cracks. With visible-dye penetrants, the bright color contrasts sharply with that of the developer, revealing cracks as a line on the surface. Fluorescent penetrants are examined under ultraviolet light for cracks. A variety of materials, with and without separate developers, is used. The sensitivity of the process can be controlled through the surface tension and viscosity of the penetrant.

The liquid penetrant NDE process can be made fairly simple. Excellent results are obtained with equipment that consists of three different spray cans, a brush, and some rags. The process has been automated for surface-cracking inspections in nuclear power plants and other hazardous applications. The results are viewed by remote closed-circuit television in these situations.

If it becomes important to inspect damaged tank cars for fine surface cracking that is not readily visible to the eye with slight magnification, liquid penetrant testing would be the method of choice because of the ease with which good results can be obtained under the conditions contemplated. The technique is superior, for this application, to the other surface inspection methods considered. The drawbacks are that it would be difficult and expensive to automate for remote sensing due to the unpredictable geometry of damaged areas, and that it cannot be used when there are tightly adhering coatings of paint. (These would have to be removed first, without "smearing" metal over crack openings.)

2.2.7 Other Surface Inspection Techniques

There are other NDE techniques for inspecting surfaces for cracking. If one simply measures the electrical impedance between two probes, using the part to carry either alternating or direct current, one can infer the presence of defects in a manner that is similar to that described for eddy currents. The technique has similar limitations to eddy currents and, in

addition, is very sensitive to the electrical characteristics of the contact between the probe and the part being examined. Conductivity measurements would seem to have few, if any, advantages over other methods and several drawbacks.

It is possible to detect defects at and near the surface by their effects on the microwave reflectivity of the surface and the phase changes these cause. Applications are primarily in large aerospace components. Sensitivity is not as great as one would like for the kinds of defects envisioned in the damaged tank car problem, and equipment needs appear to be large and out of proportion to the usefulness in this application.

Laser interferometry has also been used to detect defects, both on and near the surface and at depth in a structure. One first illuminates the area with a coherent, narrowband laser and makes the first exposure of a hologram. Then the part is stressed, either hydrostatically or simply by local heating of a few degrees. The two exposures produce interference fringes which describe the surface. Small differential movements of fractions of micrometers across a crack show up as easily recognizable changes in the fringe pattern. Equipment needs would be relatively large, and development work would be necessary to put the method into the field under emergency conditions. The one advantage of the method is that it is potentially possible to examine for cracks and defects from a distance.

2.2.8 Radiography

Radiography is a large and useful NDE discipline. It will be discussed here in terms of various combinations of radiation sources, detectors, and information extraction techniques. The basis for the technique is the fact that high-energy electromagnetic radiation (in the x-ray and gamma-ray regions of the spectrum) is attenuated differentially in passing through material objects. At a given energy, the attenuation is proportional to the total electron density along a ray from source to detector traversed by the x- or gamma-ray. Denser or thicker regions

attenuate more than lighter or thinner ones. The two-dimensional attenuation pattern on the detector forms an image which is, in effect, a shadowgram of the objects between the source and detector.

In the familiar medical or dental radiography, the source is an x-ray tube and the detector is film. The pattern on the film reveals details of hidden structures.

Because of the way in which the shadowgram image is formed by differential attenuation, radiography is not a very effective method for detecting cracks; to be detected by radiography the plane of a tight crack must lie nearly parallel to the line between source and detector. Randomly oriented cracks will seldom fulfill this condition.

In industrial applications, radiography is used primarily for verifying workmanship and integrity of weldments. Most welding faults and defects, except cracking, are readily observable. Nearly all construction codes and standards call for radiographic inspection at one or more stages of manufacture of large engineering structures.

Most industrial applications use film as the detecting medium. Depending on the application, film is exposed and processed in sizes ranging from small pieces to very long rolls. Film is usually interpreted visually.

Since the process usually involves making a "shadowgram," the sharpness of the image depends on the dimensions of the source of radiation (the smaller sources giving sharper images) and on the distance between source and detector. The effective diameter of the source in an x-ray tube is usually a millimeter or two. X-ray machines, with their electrical power supplies and cooling equipment, are comparatively large. They are used primarily in applications where the parts to be examined can be brought to the machine, though there are a number of exceptions.

Many industrial applications require that the source be brought to the part being examined, and that the equipment be significantly smaller than

is possible with an x-ray machine. In this case the source is a small capsule of a radioactive isotope which gives off gamma rays. This type of source is necessarily significantly larger than the effective source in an x-ray tube, and the output is usually much less, requiring longer exposures.

Film is expensive and its processing is time consuming. In many large-volume operations and some special-purpose applications, the cost is reduced and results improved by making the detector a phosphor, sometimes with electronic image intensification. Radiographic viewing becomes a real-time process, where the object being viewed can be moved for investigation of particular areas. Systems of this type have been developed by EG&G Idaho at the Idaho National Engineering Laboratory for inspecting the contents of large numbers of drums containing low-level nuclear wastes.

Computerized processing is used in specialized applications to enhance the diagnostic properties of images and to present radiographic information in new and unusual ways. Computerized axial tomography is an example which was developed for medical uses and is beginning to be applied to some industrial problems.

It is to be noted that the object to be radiographed is always placed between the source and the detector, and the best results are obtained when the detector is as close as possible to the object. This places severe restrictions on the usefulness of radiography in tank car assessment in the immediate field situation. Further, the limited ability of radiography to detect cracks makes its usefulness even more problematical. It does seem, however, that radiography would be useful and necessary at later stages of the operations when the tank car can be entered and is being assessed for repair, as well as during the repair operations.

2.2.9 Ultrasonics

Ultrasonics is a "classical" NDE discipline, having been used in industry since shortly after the Second World War. The field is now undergoing rapid expansion in the scope of applications; the amount and

kind of information obtained; and the precision, reproducibility, and reliability of results. This expansion comes about primarily because of the rich variety of interactions sound has with the media through which it propagates. It can provide imaging of discontinuities, such as cracks, and measurements of their dimensions and locations, along with information on the character of their surfaces. Under some conditions it can provide the same information for metallurgically disturbed but otherwise sound areas. Also, under some conditions, variations in the speed of sound and in the frequency content of ultrasonic signals can be related to more subtle metallurgical properties, such as degree of work hardening, grain-size variations, and even some of the parameters affecting fracture toughness. Further, ultrasonic techniques lend themselves to easily field-deployable analysis systems of significant sophistication for solving these types of problems in real time or near-real time. EG&G Idaho has been an industry leader in this field. Some of these latter possibilities are currently the subject of extensive research efforts by EG&G Idaho and others, and have potential application to tank car assessment.

Ultrasound is usually generated in short pulses by a piezoelectric transducer. Frequencies commonly range from about a half megahertz to perhaps ten or twenty megahertz. Sound is detected by the same or companion transducers. The most used technique is a pulse-echo method similar to sonar or radar. A pulse is sent out and its echo is evaluated in terms of time of arrival (distance to target), echo amplitude, frequency content, and phase relations. Transducers are scanned over the part to build up information on the three-dimensional relations within the part.

According to well-understood principles, sound is reflected or scattered from any location where there is a change or discontinuity in the product of the speed of sound in the material times the material density. Hence cracks, which are discontinuities in both terms, are readily detectable. Metallurgical damage without cracking can also change one or both terms in the equation; these effects are more subtle, but often observable. The wavelength of sound compared to target size is an important parameter which modifies the scattering and reflection interactions so as to carry additional and very useful information.

It has been demonstrated that small, fieldable systems based on computer techniques are capable of extracting, analyzing, and presenting the results of ultrasonic testing quickly in easily usable form. Such systems have been in use at EG&G Idaho for inservice inspection since 1977. These systems are readily adaptable in the field to a wide variety of techniques.

Because of the wide variety of useful information which can be obtained quickly in the field and the ability to operate remotely, if necessary (once the tank car has been approached to emplace the scanning device), ultrasonic techniques appear to have great potential for detailed evaluation of damaged tank cars.

2.2.10 Other NDE Techniques

This brief survey by no means exhausts the field of NDE techniques which may have potential for application in the damaged tank car problem. It does include, however, those techniques which meet the constraints of sufficient state of development, use of the field-observable quantities, rapidity of results, and ability to be used in the field under emergency conditions.

Other techniques with no or quite limited usefulness for the problem in question include neutron radiography (which obeys significantly different attenuation and scattering laws than do x- and gamma-rays, is difficult to use in the field, and will not supply additional needed information), liquid crystals and similar materials for measuring local temperature distributions (which require contact with the car to be useful), helium leak testing (very sensitive, but requires access to the interior of the car), and various techniques using radioisotopes which emit alpha or beta rays (useful in interrogating thin layers and surface coatings, but not of large importance to this problem).

2.3 NDE Survey Conclusions

Based on this survey, the following NDE techniques appear to be the most promising for on-scene evaluation of damaged tank cars. These conclusions are tentative. As the work proceeds, increased knowledge of the tank car problem may cause an adjustment in this evaluation.

1. The NDE techniques suitable for the initial remote assessment and for determining the safety of approaching the tank car are:
 - a. Supported visual observation and inspection, as defined. These determine gross conditions of damage, determine and measure larger deformations, and assess general condition and safety.
 - b. Infrared imaging. Determine existence, location, and relative sizes of significant leaks.
2. The NDE techniques for detailed assessments at close range or in contact with the damaged tank car are:
 - a. Supported visual examination. Find finer details and general observations not possible from remote location.
 - b. Ultrasonics. Make thickness measurements as an index to local deformation, detect cracks and related defects in critical and/or deformed areas, and (potentially) parameters related to metallurgical variables of concern to safety of further operations.
 - c. Acoustic Emission. Installed immediately on close approach; detect small leaks, changes in leak rates, crack movements, and movements and changes in structures that may signal the onset of increased hazards--a safety device.

- d. Liquid Penetrant Inspection. Detect surface cracking (primarily on convex deformations) that may be related to structural weakness; a secondary technique on first approach, but easy to use and potentially most useful at the later stages of the operation.

It should be noted that ultrasonic and acoustic emission sensing can be operated remotely if necessary from the same basic system, once the scanning devices and fixtures have been emplaced.

- 3. NOE techniques potentially useful after unloading and during recovery operations:
 - a. Liquid penetrant inspection to detect surface-breaking defects on accessible surfaces. (These are quicker and more precise, where applicable, than ultrasonics or radiography, and require less equipment.)
 - b. Ultrasonics to detect buried flaws and defects and those breaking on inaccessible surfaces.
 - c. Acoustic emission to detect and pinpoint structural responses to changes in loading and stress as the car is being unladen or moved.

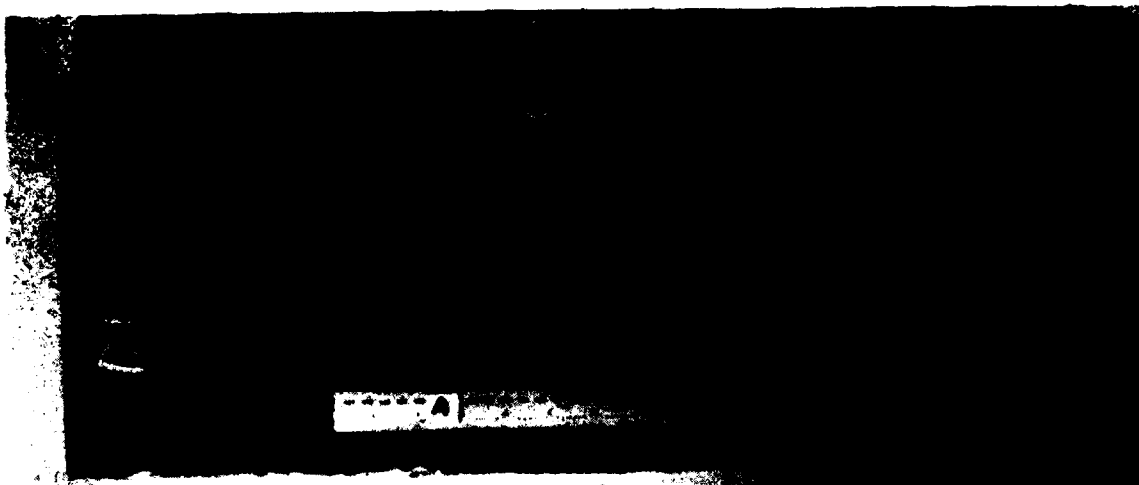
3. NDE EVALUATION OF FLAT PLATE SPECIMENS

The work described in this Section was undertaken as a reconnaissance survey to determine the techniques that would be needed and to establish an agenda for further work, if the survey gave promising results.

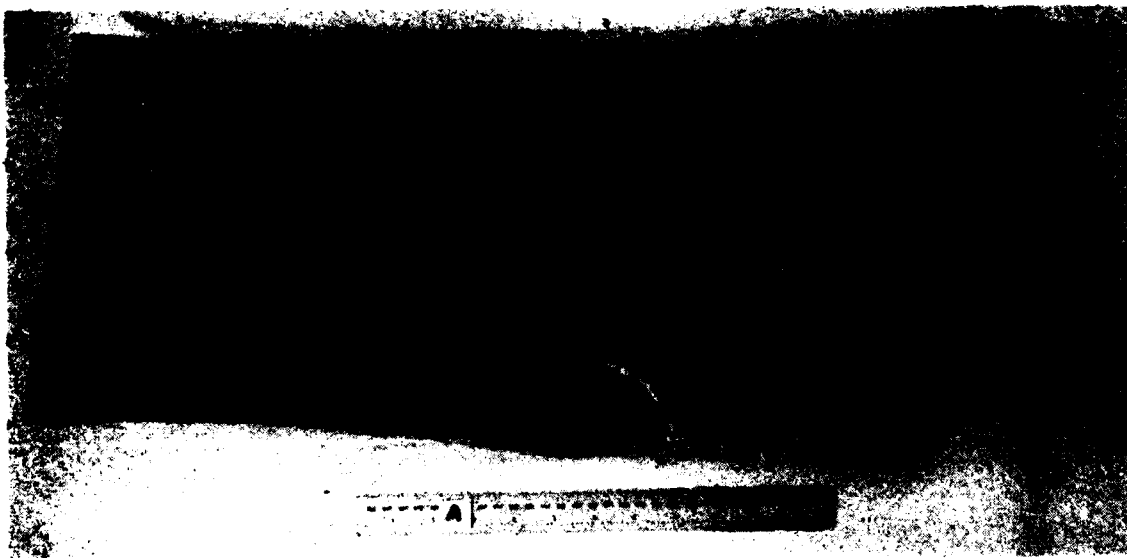
Ten deformed flat plate specimens were furnished to EG&G Idaho for nondestructive evaluation. The specimens simulated damaged areas of tank cars ranging from mildly deformed through visible fractures and tears. They were made of ASTM A-515 Grade 70 steel which exceeded the minimum standards required in the construction of railroad tanks cars. The plates were 1.59 cm (5/8 in.) thick and 61.0 cm (24 in.) square. The hemispherical tups which had been used to impact the plates were of three sizes--5.08 cm (2 in.), 9.53 cm (3.75 in.), and 14.0 cm (5.5 in.) diameters. The plates were impacted as they rested on top of a die. Four different die diameters were used: 15.2 cm (6.0 in.), 21.0 cm (8.25 in.), 27.9 cm (11.0 in.), and 34.9 cm (13.75 in.). Photographs of one of the plates are shown in Figure 1.

The approach was to measure deformation parameters using NDE techniques and attempt to correlate these parameters with physical and metallurgical measurements of damage and residual structural strength. The rationale for this approach is that if reasonable correlations can be found, then remote observations may be used to establish probabilistic bounds on the structural integrity of a derailed tank car. The bounds could be narrowed in successive stages as personnel approach closer to the car, since the shorter distances would allow them to make successively finer and more detailed measurements.

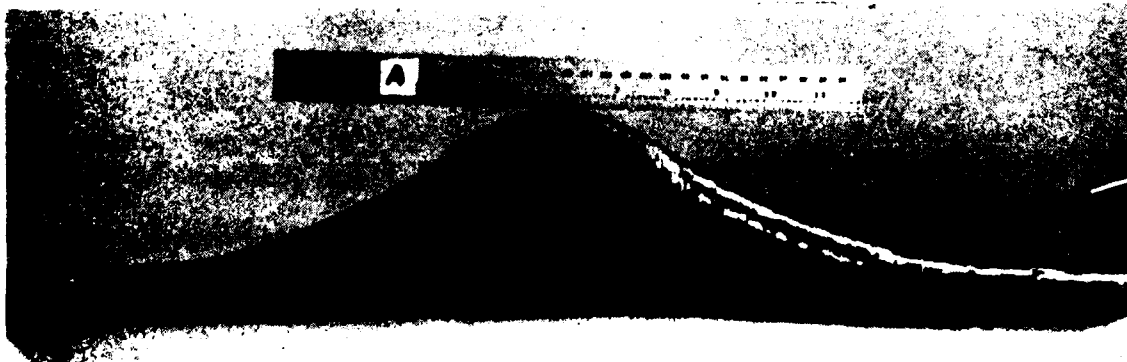
A variety of nondestructive examinations were applied, including visual inspection, liquid penetrant inspection, and various ultrasonic techniques, each under those conditions for which it was appropriate. Encouraging correlations were obtained between the degree of surface cracking and the various measures of deformation.



a. Convex (bottom) Side



b. Impact Side



c. Cross-Section

Figure 1. Three Views of a Flat Plate Specimen Showing General Dent Shape

It was observed that all of the surface cracks run in the rolling direction. This may indicate that the manufacturing process contributes to a strength problem. The depth and radius of curvature of each deformed area were measured. Figure 2 is an example of plots that were made of dent depth as a function of position. These measurements would probably be conducted remotely when in the field.

An ultrasonic thickness gauge was used to measure the thickness of all areas on the specimens. Plots were prepared of thickness as a function of position. Figure 3 is an example. It was noted that the fractures and tears which were easily found in the visual examination were located in those areas with the greatest amount of thinning. Section thinning as much as 32% was observed. Typical areas of severe thinning, which consist of two lobes on the thickness plot of a plate specimen, are shown in Figure 4. Figure 5 shows a thickness plot of a plate specimen which was not deformed enough to possess areas of severe thinning. Severe thinning points to areas where structural strengths are in question. (Additional data are given in Appendix A.)

Liquid penetrant inspections were done on both the convex and concave sides of the ten plate specimens to determine the degree of surface cracking. A map was made for each specimen showing both size and location of all surface cracks and tears. This inspection showed no signs of cracking on the concave sides of the dents except for the tears when the total thickness was penetrated; therefore, only maps of the convex sides are included. Figure 6 is an example of these maps.

The total length of surface cracks, number of surface cracks, and the area showing significant surface cracking were taken from each map. Statistical analysis shows excellent correlations between the degree of surface cracking and various measures of deformation. The measures of surface cracking and deformation compared are listed with their correlation coefficients in Table 1. Plots of area of surface cracking versus percent reduction in thickness, area of surface cracking versus maximum depth

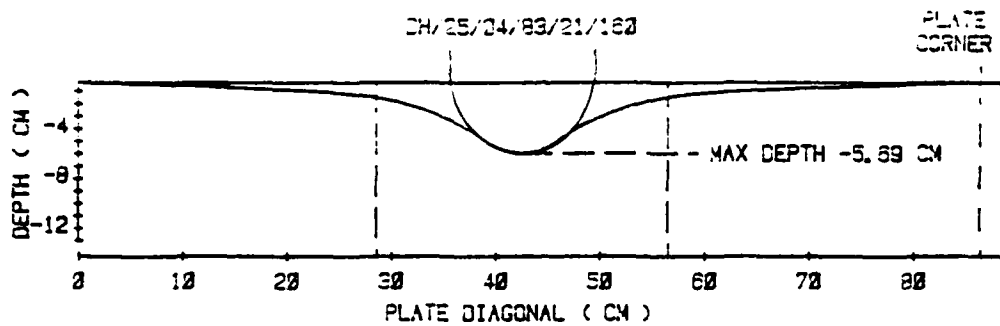


Figure 2. Dial Micrometer Measurements of Dent Depth

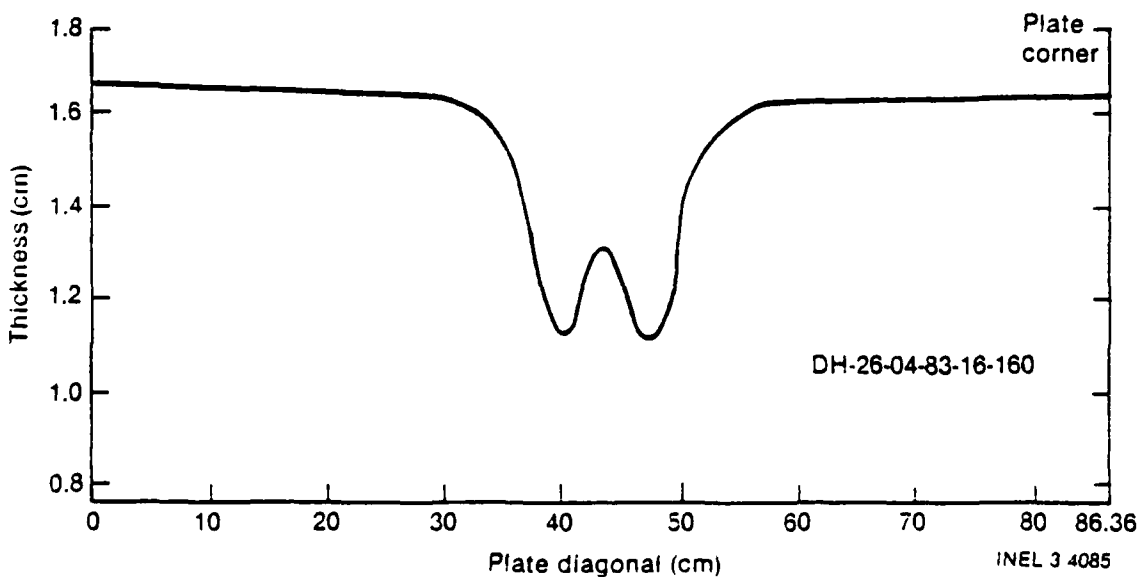


Figure 3. Typical Plot of Thickness Versus Position Obtained by Use of Ultrasonic Thickness Gauge (Plate No. DH-26-04-83-16-160)

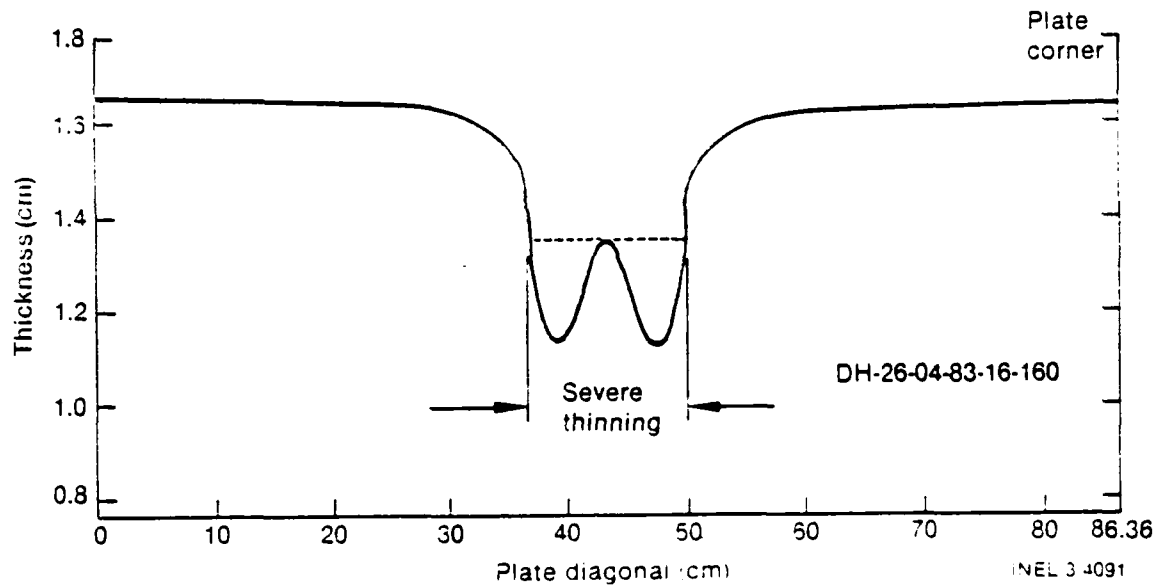


Figure 4. Thickness Plot Showing Severe Thinning of a Plate Specimen

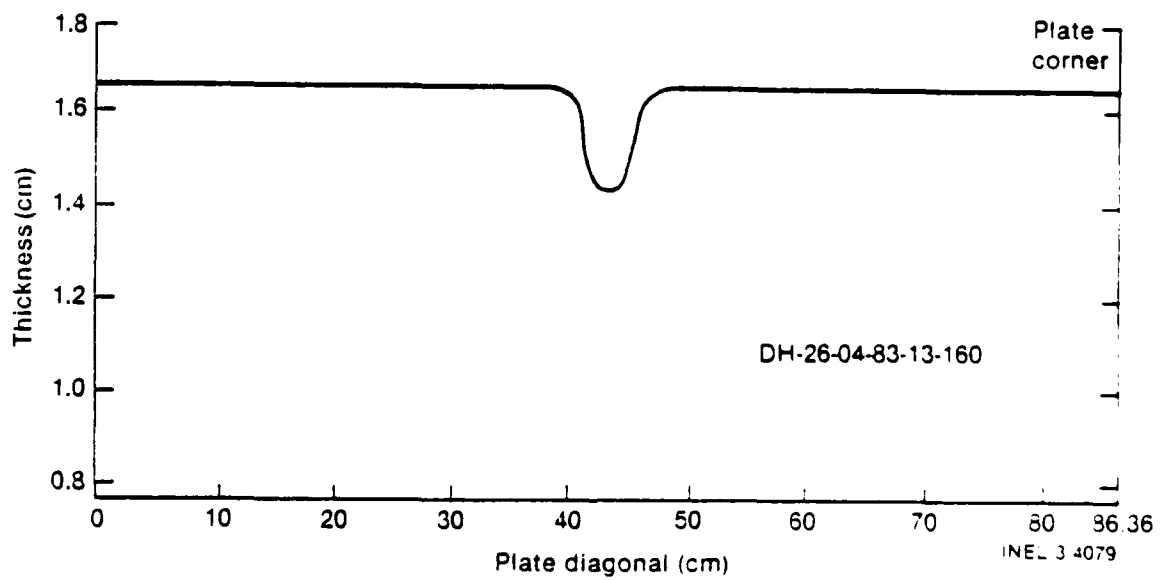


Figure 5. Thickness Plot for Plate Specimen Which Was Not Deformed Enough to Possess Severe Thinning

DH-25-04-83-14-160



Figure 6. Typical Map of Surface Cracks on the Convex (Bottom) Side of a Flat Plate Specimen

TABLE 1. CORRELATION OF MEASURES OF DEGREE OF SURFACE CRACKING AND DEFORMATION

Measure of Surface Cracking	Measure of Deformation	Y-Intercept	Slope	Correlation Coefficient
Total length of cracks	%Reduction in thickness	-7.86 cm	1.04 cm/% reduction	0.5409
Area of surface cracking	%Reduction in thickness	-49.33 cm ²	10.44 cm ² / % reduction	0.6921
Total length of cracks	Dent depth	-4.05 cm	3.12 cm/cm	0.6075
Number of cracks	Dent depth	-4.24 cracks	11.45 cracks/cm	0.7039
Area of surface cracking	Dent depth	-8.66 cm ²	31.04 cm ² /cm	0.8698
Total length of cracks	Radius of curvature	-5.72 cm	3.75 cm/cm	0.5486
Number of cracks	Radius of curvature	-37.08 cracks	18.30 cracks/cm	0.7472
Area of surface cracking	Radius of curvature	-90.59 cm ²	48.39 cm ² /cm	0.9010

of dent, number of cracks versus maximum depth of dent, and total length of cracks versus maximum depth of dent are given in Figures 7 through 10.

Although the correlations between some of the measures of surface cracking and deformation are excellent, these correlations are based on a small number of samples of one type of tank car material. If the correlations hold up statistically with additional specimens and denting modes, and if the cracking can be related reliably to adverse changes in mechanical properties, then a very valuable tool will be available for assessing structural integrity of damaged tank cars through remotely-made measurements of deformation.

A computer-controlled ultrasonic imaging system was used for immersed ultrasonic testing of the plates. Figure 11 shows a plate being examined using this system. Ultrasonic inspections were used to locate areas of distressed metal. These areas were assumed to

- o be near known cracks
- o be in otherwise "sound metal" (middle third of thickness)
- o have relatively stronger echo signals at high frequencies than low frequencies
- o have the same orientation as known cracks (which indicate stress directions).

These properties were postulated for areas which contain severely disturbed metallurgy, where the part may be on the verge of outright rupture. One would expect that the deformation, plastic flow, and/or formation of incipient shear bands would change the grain structure and acoustic impedance in such a way that partial reflections could be obtained; the short lengths characteristic of the deformation structures would favor reflections at higher frequencies (shorter wavelengths). The assumptions of proximity to and orientation similar to known ruptures are simply

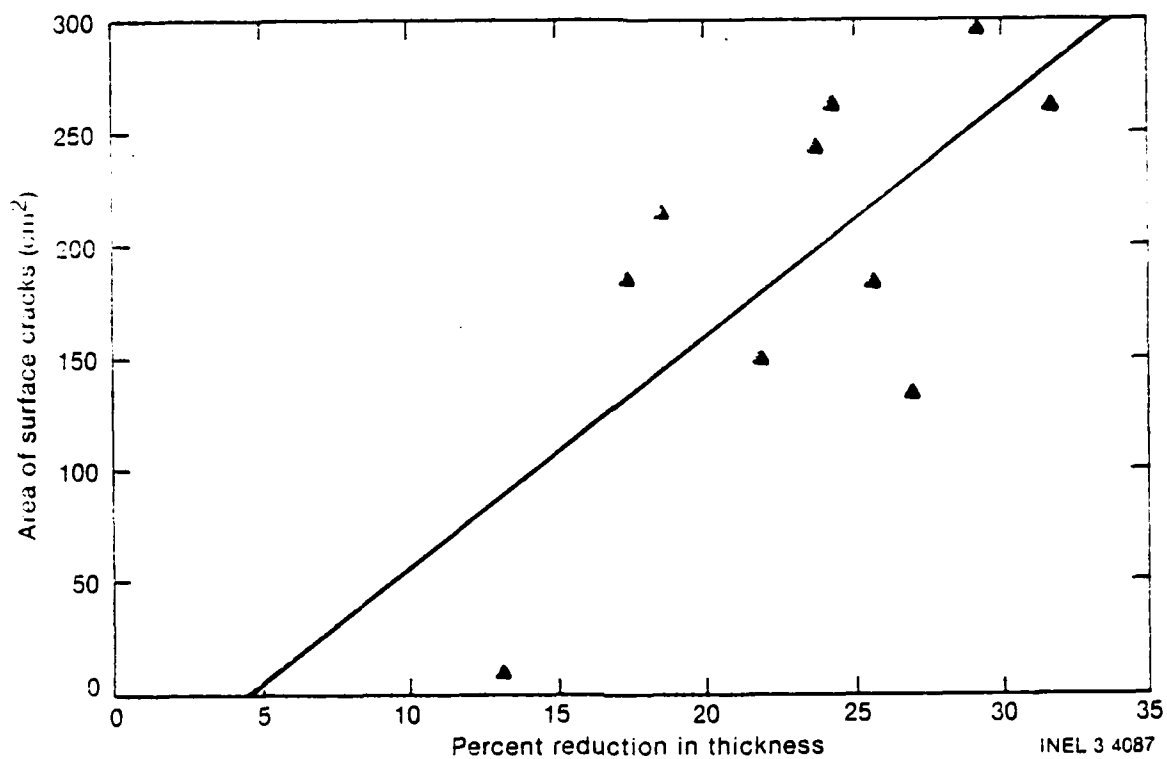


Figure 7. Area of Surface Cracking as a Function of Percent Reduction in Thickness

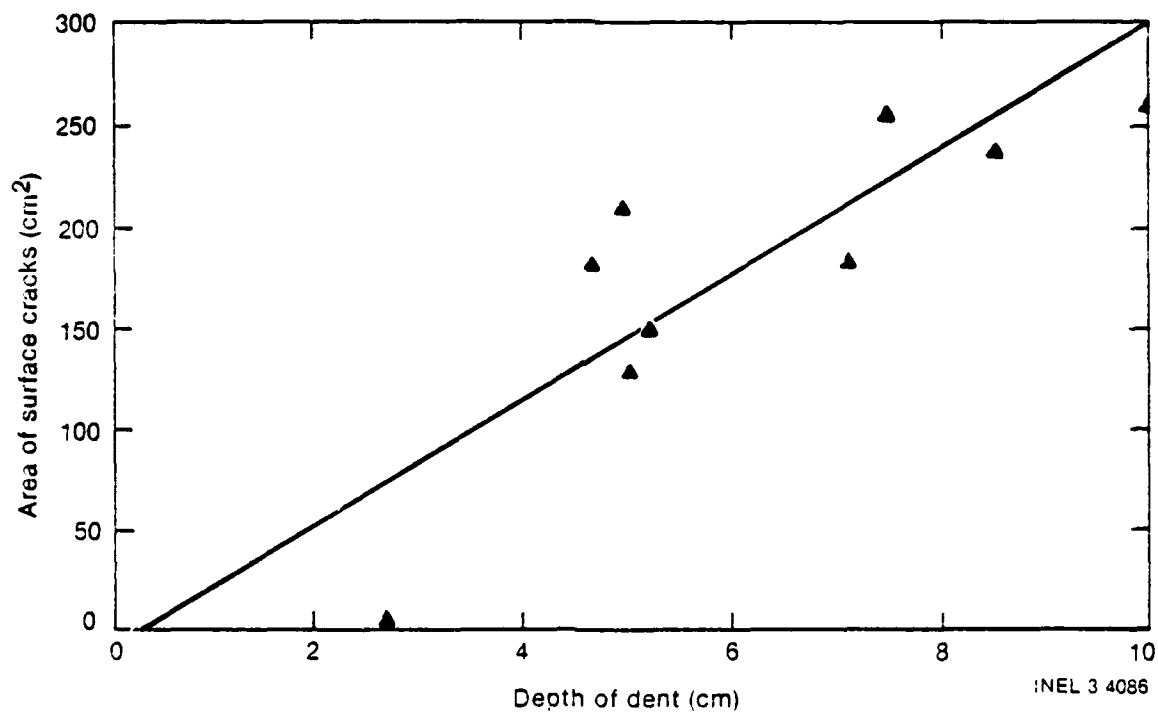


Figure 8. Area of Surface Cracking as a Function of Dent Depth

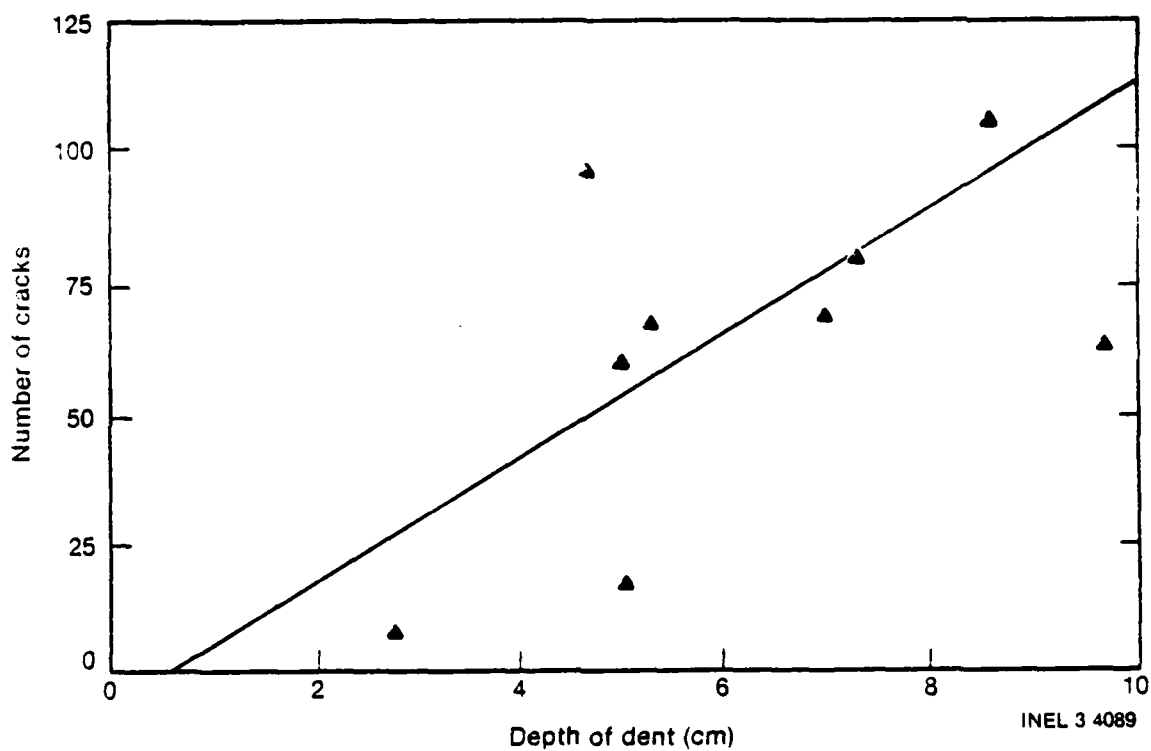


Figure 9. Number of Cracks as a Function of Dent Depth

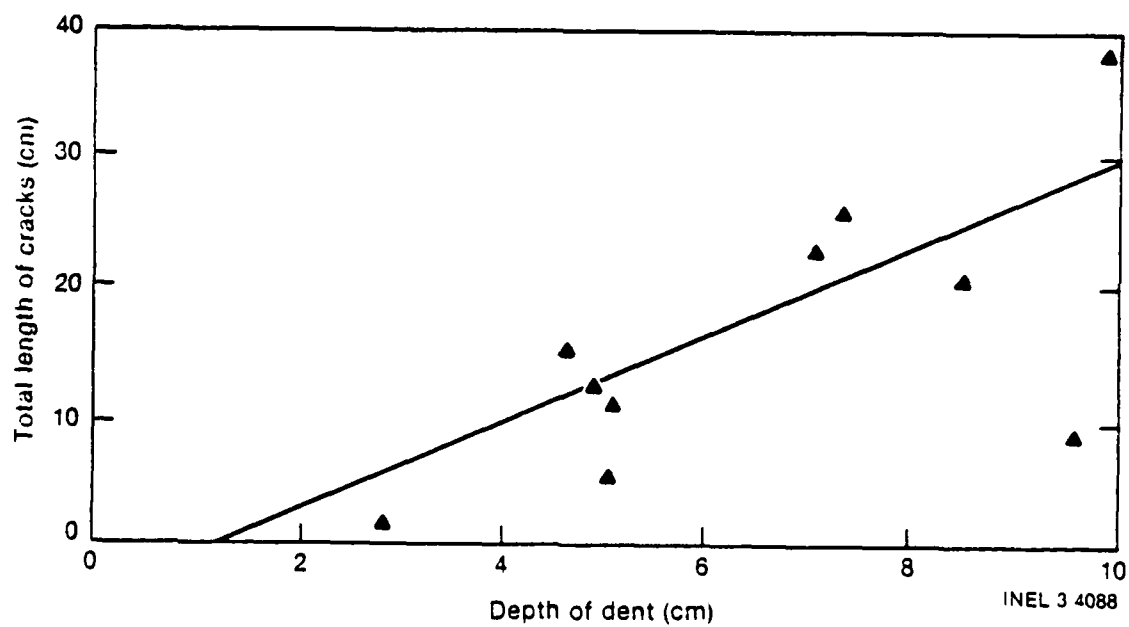


Figure 10. Total Length of Cracks as a Function of Dent Depth



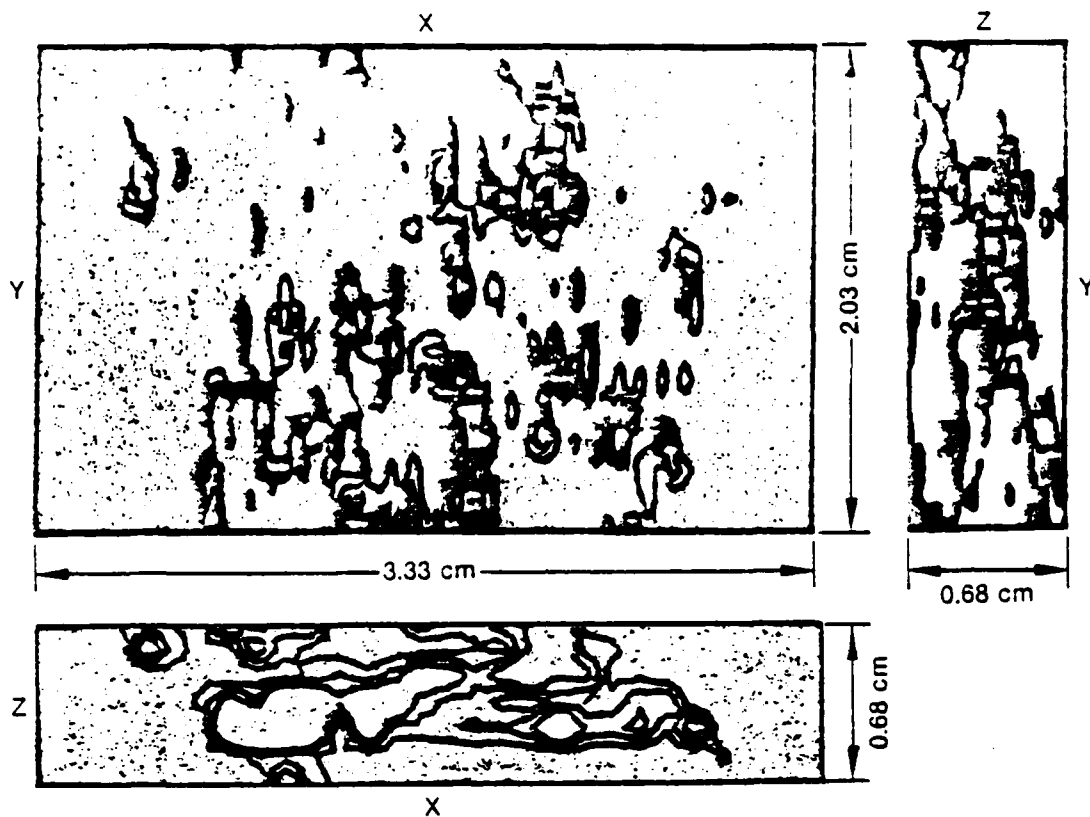
Figure 11. Ultrasonic Examination of Flat Plate Specimen

experimental conveniences to narrow the areas to be investigated. The confinement of the search to targets that do not break the surface ("sound metal") was intended to steer the investigation away from obvious cracks.

The initial ultrasonic measurements were made by scanning at a frequency of 2.25 MHz, followed by computer-generated imaging for interpretation. No definite indications meeting the postulated conditions were found. Succeeding measurements concentrated on areas parallel to and displaced from the centers of the largest ruptures. Targets meeting the postulated conditions were found in these areas (see Figure 12). They seem likely to represent the postulated zones of high mechanical disturbance on the verge of failure. Additional ultrasonic work, followed by careful metallography, is needed to confirm this identification.

In addition, small point-like targets, and some of slightly extended areas, were found in moderately deformed areas. This class of targets was entirely absent in areas of little or no deformation, indicating that the targets are associated with deformation. The determination of their exact nature requires a more detailed investigation.

If further work confirms the preliminary interpretation of the extended and point-like targets as representing severe and moderate damage, respectively, preceding failure, and if the same or similar phenomena are found in other tank car materials, then ultrasonic measurements made in situ on damaged tank cars will be a powerful tool for assessing tank car status in the field. It is conclusive, however, that these targets do point to areas of deformation where fracture toughness and strength parameters should be investigated for possible correlation with field-observable quantities.



DH-26-04-83-16-160
Scan #091

These contour plots were generated by the ultrasonic imaging system. The system produces maps of the part in which the contours are lines of equal reflected sonic intensity. One reads these maps much like a standard topographic map; the patterns made by the reflected sound are the "hills" of the topographic map giving a sonic picture of the flaw. The x-y plane is the top view of a small area of a plate specimen. The x-z and the y-z planes are two different views of the thickness of the same area (Plate Number DH-26-04-83-16-160).

Figure 12. Contour Plots Generated by the Ultrasonic Imaging System of Flaws in Metal

4. FRACTURE MECHANICS

Tank car failures result from an interaction between defects (cracks) and stress which can be quantified using linear-elastic fracture mechanics (LEFM). A brief explanation of fracture mechanics is provided here along with sample analyses corresponding to damaged and undamaged tank cars. The interested reader is referred to References 4-6 for additional information on fracture mechanics.

Failure occurs when K_I (applied stress intensity factor) equals K_{IC} (plane strain fracture toughness). K_I is a function of the applied stress (σ) and the crack depth (a) as shown in Equation 1:

$$K_I = Y \sigma (a)^{1/2}, \quad (1)$$

where Y is a geometric parameter. K_{IC} is a material property which may vary as a function of temperature, strain rate, the heat of the specific material, etc. Therefore, for accurate predictions of structural integrity, it is necessary to know K_{IC} for the stock from which the component of concern was fabricated. In many instances this is not possible, so estimates of the lower limit of K_{IC} for the type of material (to be on the conservative side of a failure prediction) are used to assess structural integrity.

The plates of ASTM A515 Grade 70 steel, which were already examined non-destructively, were used to illustrate an approach based on fracture mechanics that can be used to estimate tank car structural integrity. This discussion is separated into the following subsections: Estimation of Fracture Toughness, Calculation of Failure Condition, Discussion, and Results and Conclusions.

⁴ R. W. Hertzberg, Deformation and Fracture Mechanics of Engineering Materials, 2nd Edition, New York, John Wiley and Sons, 1983.

⁵ A. S. Tetelman and A. J. McEvily, Jr., Fracture of Structural Materials, New York, John Wiley and Sons, 1967.

⁶ S. T. Rolfe and J. M. Barsom, Fracture and Fatigue Control in Structures, Applications of Fracture Mechanics, New Jersey, Prentice-Hall, Inc., 1977.

4.1 Estimates of Fracture Toughness

The DOT specifications for ASTM A515 Grade 70 (A515-70) steel for use in the construction of railroad tank cars do not require that the material meet a minimum fracture toughness parameter, i.e., a minimum Charpy V-notch (CVN) impact energy, nil-ductility transition temperature (NDTT), K_{IC} , etc, as a function of the minimum operating temperature. (The chemical and mechanical property requirements are given in Table 2.)^{7,3} Since the DOT specifications do not contain any minimum requirements for fracture toughness, a literature search was conducted to develop a data base for A515-70. The data base was to include CVN, NDTT, and fracture toughness measurements for temperatures ranging from 211 to 344 K (-80 to 160°F) for base metal and weldments. The results of this literature search showed that these data are not available. This has since been confirmed in discussions with representatives of steel companies.⁹⁻¹¹ The only data obtained were NDTT of 294 K (70°F) for two heats of A515-70 and Dynamic Tear results for test temperatures ranging from 227 to 339 K (-50 to 150 °F).¹²⁻¹⁴

⁷ Annual Book of ASTM Standards, Part 4, 1981.

⁸ "Hazardous Materials Regulations of the Department of Transportation," Tariff No. BOF-6000-B, Subpart C, pp. 512-514, United States Government Printing Office, December 22, 1981.

⁹ A. Wilson, Lukens Steel Co., Coatesville, PA, Private Communication to M. A. Tupper, EG&G Idaho, September 15, 1983.

¹⁰ R. Brown, United States Steel, Pittsburgh, PA, Private Communication to M. A. Tupper, EG&G Idaho, September 15, 1983.

¹¹ C. D. Spaeder, U.S. Steel Research, Pittsburgh, PA, Private Communication to M. A. Tupper, EG&G Idaho, September 15, 1983.

¹² O. W. Albritton, "Avoiding Brittle Fracture in Cold Formed ASTM A515 Steel - Metal Progress," pp. 115-120, September 1970.

¹³ W. W. Pellini, R. D. Eiber, and L. L. Olson, "Phase 03 Report on Fracture Properties of Tank Car Steels - Characterization and Analysis," Report No. RA-03-4-32, RPI-AAR, Tank Car Safety Research and Test Project, August 20, 1975.

¹⁴ J. C. Newman, Jr. and S. Raju, "Analysis of Surface Cracks in Finite Plates Under Tension or Bending Loads," NASA Technical Paper 1578, December 1979.

TABLE 2. CHEMISTRY AND MECHANICAL PROPERTIES OF ASTM A-515 GRADE 70 STEEL

Steel	Chemistry (wt%)				Yield Strength (MPa) (ksi)	Ultimate Strength (MPa) (ksi)	Minimum Elongation	
	C	Mn	P	S			In 203 mm (8 in.) (%)	In 50.8 mm (2 in.) (%)
A-515 Grade 70 5/8 in. plates ^a	0.28	0.83	0.013	0.027	0.24	503.7	24	
A-515 Grade 70 ASTM requirements	0.31, max	0.90	0.035, max	0.04, max	0.13-0.33	262.2 min 483-621	17	21

a. Certification results for heat No. Y54741 SL3-4 were used in this evaluation of 5/8-in. plates. The Department of Transportation allows a maximum of 0.31 carbon and requires a minimum of 483 MPa (70 ksi) in the welded condition, and 20% minimum elongation in 50.8 mm (2 in.).

Because of the lack of data, two plates from the ten supplied to EG&G Idaho were used to estimate the fracture toughness of the undeformed and the deformed material. Figures 13 and 14 provide schematics of the two plates showing the thickness measurements and the location of test specimens. Because of time and material limitations, it was not possible to develop valid plane strain fracture toughness (K_{IC}) measurements. Therefore, estimates of K_{IC} were made using the true stress-true strain curve developed from tensile specimens (Table 3). These tests were conducted at 294 K (70°F), and it is not possible at this time to identify if the change in K_{IC} is due to an increase in NDTT or a decrease in the upper shelf value.

4.1.1 Calculations of Fracture Conditions

The limited data from the literature suggest that NDTT > -60°F, which means that brittle fracture could occur under normal operating conditions. The substantial reduction in K_{IC} (Table 3) and the development of cracks due to deformation suggest that the possibility of catastrophic failure is substantially greater for a damaged tank car than for an undamaged car. This section illustrates the use of LEFM concepts for predicting conditions for failure and identifies areas where additional work is required.

If sufficient fracture toughness, K_{IC} , data versus test temperature had been available for A515-70, a statistical analysis would have been conducted to establish a lower bound using an acceptable probability of overestimating K_{IC} . Since these data were not available, the experimental estimates of K_{IC} in Table 3 were used for this analysis. From Equation 1 it is apparent that crack size and stress interact to determine K_I , e.g., for a small stress it requires a substantial flaw size for $K_I = K_{IC}$. The DOT specification does not identify an upper limit for the design stress; therefore, for illustrative purposes it is assumed that the design stress is at least as low as the smaller of 1/3 ultimate tensile strength (σ_{uts}) or 2/3 yield strength (σ_{ys}), which corresponds to 161 MPa (23.3 ksi) for A515-70.⁶

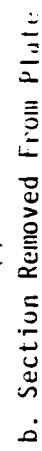
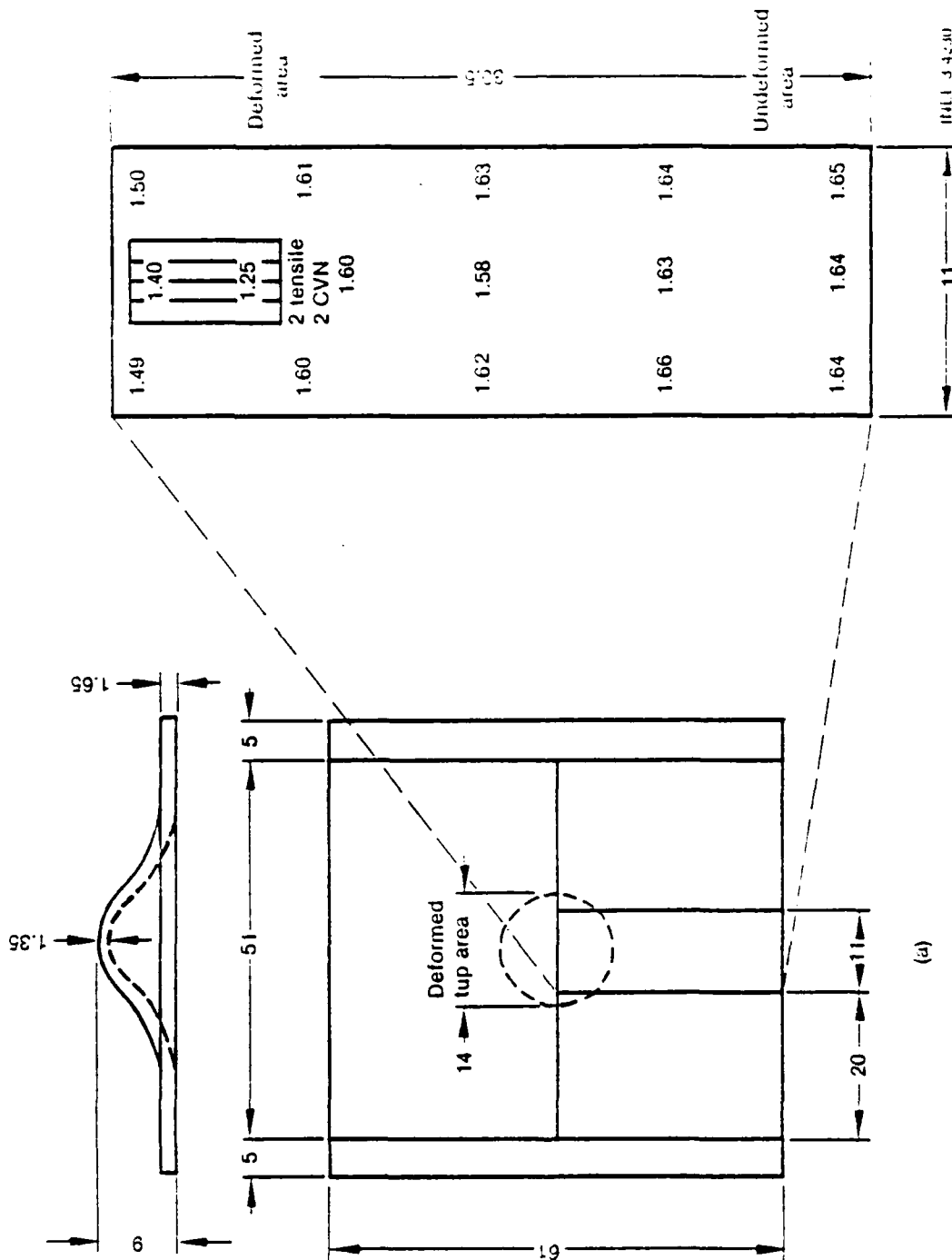


Figure 13. Thickness Measurements (mm) and Location of Test Specimens Removed from Plate DII-20-14-83-16-160.



a. General Schematic

b. Section Removed From Plate

Figure 14. Thickness Measurements (mm) and Location of Test Specimens Removed from Plate DII-76-04-83-22-160

TABLE 3. MECHANICAL PROPERTIES FOR PLATES 16 AND 22

Specimen Identification	Thickness		Yield Strength		Ultimate Strength		Cold Work (%)	Estimated K_{Ic}	
	(cm)	(in.)	(MPa)	(ksi)	(MPa)	(ksi)		($\text{MPa}\cdot\text{cm}^{1/2}$)	($\text{ksi}\cdot\text{in.}^{1/2}$)
16-3	1.651	0.650	338	49	538	78	0	128	116
16-2	1.575	0.620	476	69	593	86	4.5	117	106
16-1	1.567	0.617	490	71	593	86	5.1	111	101
16-4	1.130	0.445	765	111	800	116	31.5	48	44
22-3	1.626	0.640	317	46	558	81	1.5	111	101
22-1	1.575	0.620	469	68	600	87	4.6	112	102
22-2	1.562	0.615	483	70	600	87	5.4	90	82
22-4	1.232	0.485	710	103	712	112	25.4	46	42

The defects generally encountered or postulated in a component are partial penetrating flaws either on the surface or embedded. Since surface flaws of the same size as embedded flaws are generally more detrimental, assuming each is exposed to similar stresses, only surface flaws are discussed here. Two analyses are used: one for an undamaged tank car where the critical flaw size is calculated based on the applied stress (σ_{app}) = 151 MPa (23.3 ksi), and K_{IC} = 110 MPa·m^{1/2} (100 ksi·in.^{1/2}) in Table 3, and the second for a damaged tank car where the maximum allowable stress is calculated using K_{IC} = 100 ($\frac{11}{100}$) = 44 MPa·m^{1/2} (40 ksi·in.^{1/2}) and the crack depth corresponds to those measured by NDE.

4.1.2 Critical Flaw Sizes for Undamaged Tanks

The general equation for calculating K_I (Equation 1) is not directly applicable for surface flaws. Equation 2 is frequently used for surface cracks.

$$K_I = M_I \sigma \left(\frac{a}{Q} \right)^{1/2} \quad (2)$$

where

- M = the stress-intensity boundary correction factor¹⁴
- σ = applied stress = 23.3 ksi
- a = crack depth
- Q = $1 + 1.464 (a/c)^{1.65}$ (shape factor for elliptical crack).

$$M = [M_1 + M_2 (a/t)^2 + M_3 (a/t)^4] f_s f_w g \quad (3)$$

where

$$M_1 = 1.13 - 0.09 (a/c)$$

$$M_2 = -0.54 + \frac{0.89}{0.2 + a/c}$$

$$M_3 = 0.5 - \frac{1.0}{0.65 + a/c} + 14 (1.0 - a/c)^{24}$$

$$g = 1 + [0.1 + 0.35 (a/t)^2] (1 - \sin \phi)^2$$

[ϕ is measured around the circumference of the flaw starting at $\phi = 0$ (free surface) to $\phi = 90^\circ$ (maximum depth)]

$$f_\phi = [(a/c)^2 \cos^2 \phi + \sin^2 \phi]^{1/4}$$

$$f_w = \left[\sec \frac{\pi c}{2b} (a/t)^{1/2} \right]^{1/2} \text{ (finite width correction)}$$

$$c = \text{one-half crack length}$$

$$t = \text{material thickness.}$$

Critical flaw sizes are calculated for two extremes in aspect ratio ($a/2c$) and for K_{Ic} at the free surface and at the maximum depth for the surface flaw. The correlation between applied stress and flaw sizes is given in Figure 15. This figure may be used to identify the critical crack depth for a given value of K_{Ic} .

4.1.3 Failure Conditions for a Damaged Tank Car

Equation 2 was used to calculate the critical crack depth (a) and applied stress relationship corresponding to $K_{Ic} = 33, 44, \text{ and } 55 \text{ MPa}\cdot\text{m}^{1/2}$ (30, 40, and 50 $\text{ksi}\cdot\text{in.}^{1/2}$) for the damaged tank cars of wall thickness (t) = 12.2 mm (0.48 in.). These values of K_{Ic} were selected for a sensitivity analysis. The results of these calculations are shown in Figure 16.

4.2 Discussion

The data base of fracture toughness parameters versus temperature is inadequate for developing a statistically based correlation between K_{Ic} and temperature. It was necessary to estimate K_{Ic} to illustrate the analytical approach for calculating the critical flaw depth, for undamaged tank cars, and for calculating the critical flaw depth-stress correlation for damaged tanks.

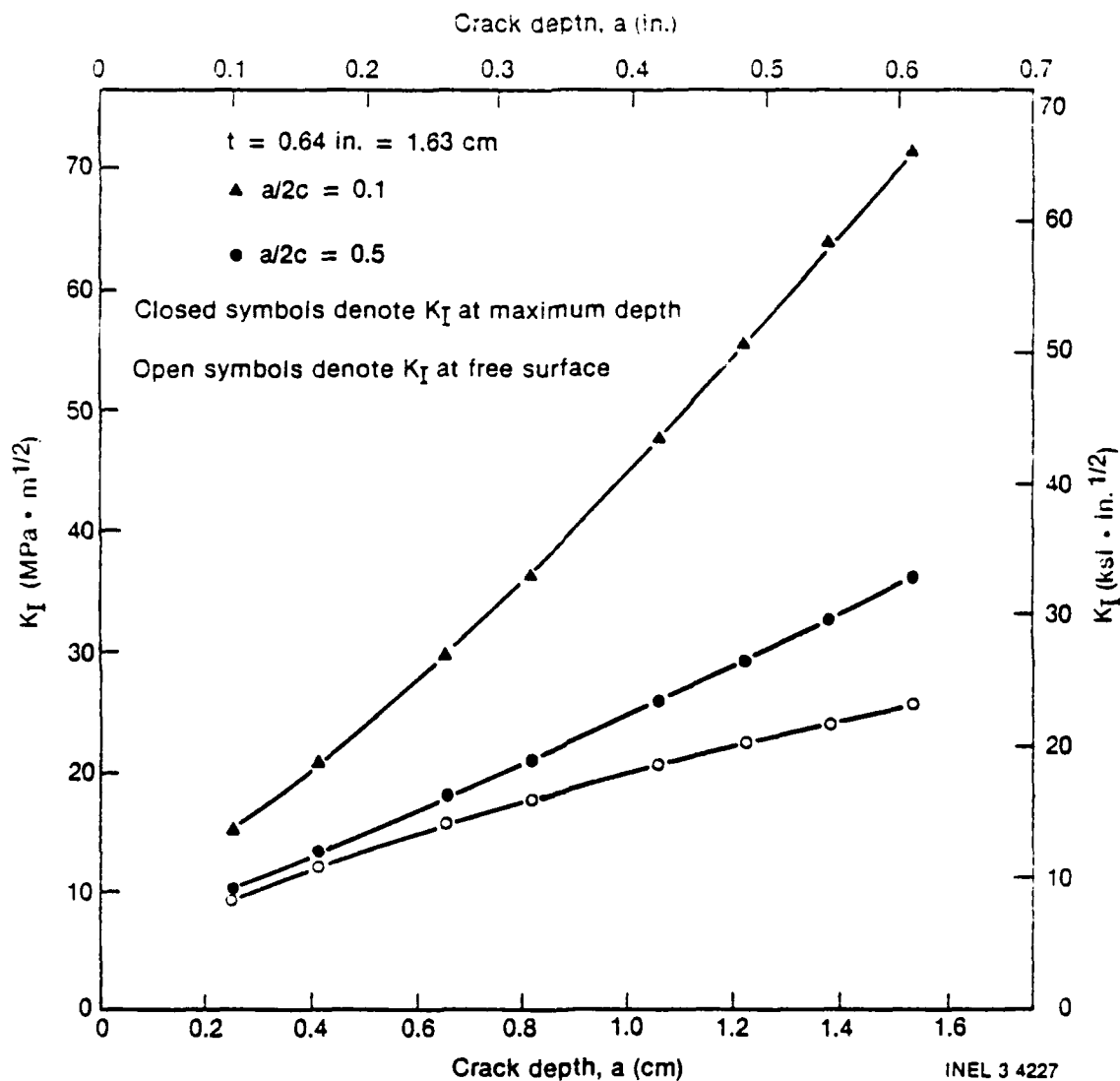


Figure 15. Correlation Between Applied Stress Intensity Factor and Crack Depth for Two Extremes in Aspect Ratio for the Undamaged Tank Car

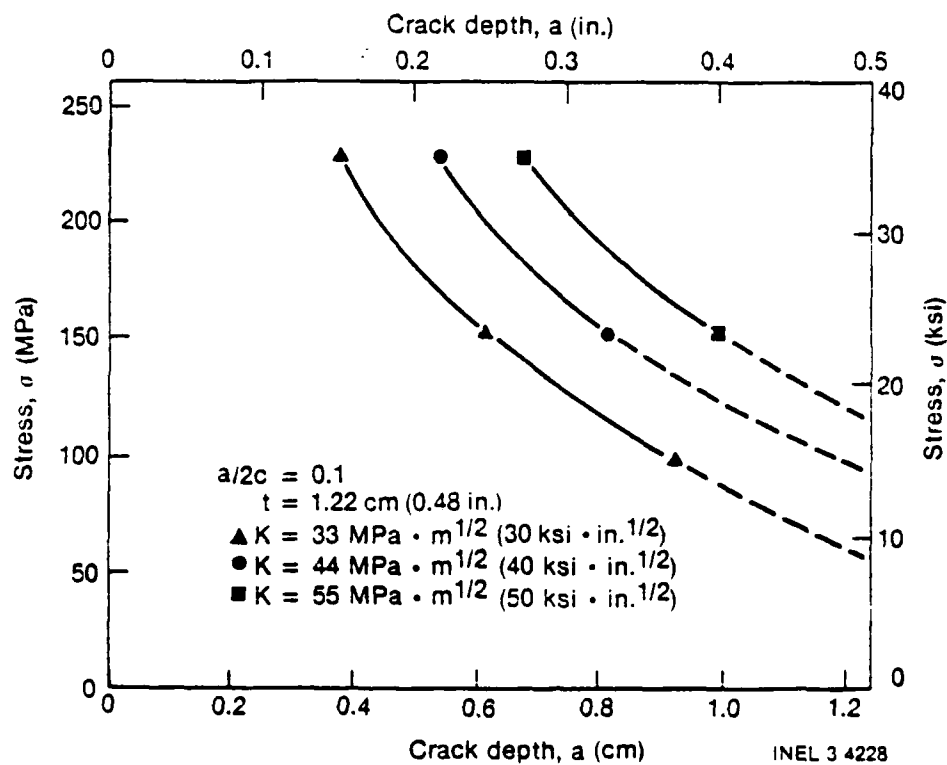


Figure 16. Correlation Between Applied Stress and Crack Depth for Three Values of K_{IC} with $a/2c = 0.1$

4.2.1 Undamaged Tank Cars

The estimate of $K_{IC} = 110 \text{ MPa}\cdot\text{m}^{1/2}$ ($100 \text{ ksi}\cdot\text{in.}^{1/2}$) in Table 3 for the undamaged tank car material at 294 K (70°F) was used to calculate the critical crack depth (i.e., that which would cause failure) if the 16.3-mm (0.64-in.) thick wall was exposed to a stress of 161 MPa (23.3 ksi). The results of these calculations are shown in Figure 15 for $a/2c = 0.1$ and $a/2c = 0.5$, where $2c$ is crack length. The peak K_I values occur at maximum depth for $a/2c = 0.1$ and at the free surface for $a/2c = 0.5$. Experimental evidence suggests that when K_I (at the free surface) = K_{IC} , crack initiation will frequently not occur due to the plane stress (as opposed to plane strain) condition at the free surface. Under plane stress conditions $K_{\text{critical}} > K_{IC}$; therefore, crack initiation occurs somewhere else around the perimeter of the crack. The curves represented by the solid triangles and the open circles in Figure 15 bound the conditions for failure. For analytical purposes, a conservative estimate was made that the failure conditions are governed by the plot for $a/2c = 0.1$ in Figure 15. The calculated conditions for failure are given in Table 4. For $a = t$, $K_I < K_{IC}$ [$110 \text{ MPa}\cdot\text{m}^{1/2}$, ($100 \text{ ksi}\cdot\text{in.}^{1/2}$)], which means the tank should leak before failure. (This does not take into consideration the stored energy in the tank car.) Figure 15 is helpful in illustrating the sensitivity of the critical crack depth to K_{IC} . For example, since References 7 and 8 do not specify any fracture toughness requirement for A515-70, it is likely that the lowest service temperature of nominally 222 K (-60°F) is less than NDTT. For this situation, $K_{IC} \sim 44 \text{ MPa}\cdot\text{m}^{1/2}$ ($40 \text{ ksi}\cdot\text{in.}^{1/2}$) corresponds to a critical crack depth (Figure 15 and Table 4) of $a = 0.99 \text{ cm}$ (0.39 in.). This is a substantial crack size which explains the relatively few failures that have occurred under normal conditions.

4.2.2 Damaged Tank Car

For the damaged tank car, where the wall thickness had been reduced 25%, Table 3 shows the estimated value of $K_{IC} = 44 \text{ MPa}\cdot\text{m}^{1/2}$ ($40 \text{ ksi}\cdot\text{in.}^{1/2}$). Figure 16 shows a plot of critical stress versus crack depth for three values of K_{IC} . An example of how these plots may be used is as follows:

TABLE 4. CALCULATED CONDITIONS FOR FRACTURE^a

Tank Car Condition	K _{Ic}		Critical Stress	Flaw Depth (a) for			
	$\frac{1}{2}$ (MPa·m)	$\frac{1}{2}$ (ksi·in.)		a/2c = 0.1		a/2c = 0.5	
			(MPa)	(ksi)	(mm)	(in.)	(in.)
Undamaged	110	100	160.8	23.3	>16.3	>0.64	--
	44	40	160.8	23.3	9.9	0.39	--
Damaged	44	40	>241.5	>35.0	1.3	0.05	--
	44	40	276.0	40.0	4.4	0.18	--
	33	30	276.0	40.0	1.3	0.05	--
	33	30	216.0	31.3	4.4	0.18	--
	44	40	372.6	54.0	--	--	6.4
	44	40	222.9	32.3	--	--	11.7
	33	30	276.0	40.0	--	--	6.4
	33	30	164.2	23.8	--	--	11.7
							0.25
							0.46
							0.25
							0.46

a. If crack depth (a) is defined, then the calculated stress is the critical stress; but if stress is given, then the calculated crack depth is a critical value.

(1) NDE revealed an estimated average crack length of 1.27 cm (0.5 in.) (disregarding the small defects) and a maximum crack length of 44.5 mm (1.75 in.) (not penetrating the wall thickness). These measurements were obtained from plates 16 and 22 where 349.3-mm (13.75-in.) and 279-mm (11.0-in.) die diameters were used, respectively, with a 140-mm (5.5-in.) tup

(2) $K_{Ic} = 44 \text{ MPa}\cdot\text{m}^{1/2}$ (40 ksi·in.^{1/2})

(3) Figure 16 shows for $a/2c = 0.1$

if $a = 0.44 \text{ cm}$ (0.175 in.), then $\sigma_{\text{critical}} \sim 102 \text{ MPa}$ (40 ksi).

It should be pointed out that the values σ_{critical} include residual plus applied stresses. If K_{Ic} is reduced from 44 to 33 MPa·m^{1/2} (40 to 30 ksi·m^{1/2}), then the critical stresses are reduced as shown in Table 4.

A similar set of curves for $a/2c = 0.5$, provided in Figure 17, are used to make a comparison of the critical stresses shown in Table 4.

For $K_{Ic} = 44 \text{ MPa}\cdot\text{m}^{1/2}$ (40 ksi·in.^{1/2}),

if $2c = 12.7 \text{ mm}$ (0.50 in.) and $a = 6.4 \text{ mm}$ (0.25 in.), then $\sigma_{\text{critical}} = 372 \text{ MPa}$ (54 ksi) which appears to be less than the extrapolated value in Figure 16 for $a/2c = 0.1$ for the same crack length

if $2c = 23.4 \text{ mm}$ (0.92 in.) and $a = 11.7 \text{ mm}$ (0.46 in.), then $\sigma_{\text{critical}} = 223 \text{ MPa}$ (32.3 ksi)

For $K_{Ic} = 33 \text{ MPa}\cdot\text{m}^{1/2}$ (30 ksi·in.^{1/2}),

if $2c = 23.4 \text{ mm}$ (0.92 in.) and $a = 11.7 \text{ mm}$ (0.46 in.), then $\sigma_{\text{critical}} = 60.5 \text{ MPa}$ (23.8 ksi).

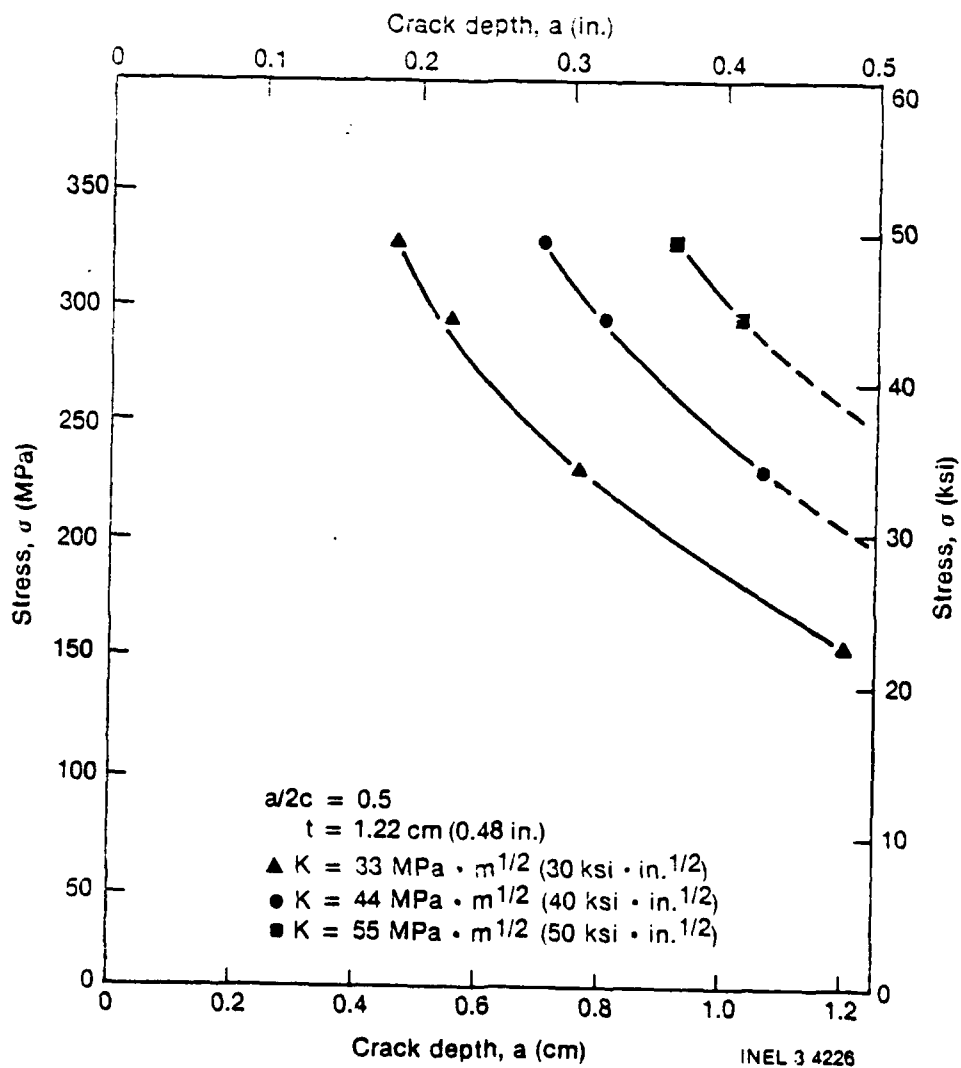


Figure 17. Correlation Between Applied Stress and Crack Depth for Three Values of K_{IC} with $a/2c = 0.5$

4.2.3 General Discussion

The above calculations illustrate the potential applicability of LEFM techniques for predicting failure conditions, e.g., structural integrity of damaged tank cars. The analyses in Sections 4.1.1 through 4.2.2 also illustrate the sensitivity of the failure criterion to K_{IC} . Therefore, it is necessary to have conservatively low estimates of K_{IC} for the undamaged material. The next requirement is to relate the change in K_{IC} as a function of deformation, which requires information regarding the magnitude of deformation for actual damaged tank cars. It would then be necessary to develop a correlation between reduction in thickness and change in K_{IC} . Because of the lack of data for A515-70, it is suggested that an alternate material be selected for evaluation.

Figure 16, which shows the sensitivity of the critical crack depth to stress, suggests the need for a stress analysis of a typical damaged tank car using different loading points and techniques on being moved. The magnitude of these stresses could then be used in conjunction with Figure 16 to estimate the accuracy needed for measurements of K_{IC} and NDE measurement of crack depth. It is likely when smaller crack sizes are considered that the predicted failure stresses will exceed the yield strength, or the stress associated with moving the damaged component will exceed the yield strength in a localized region. This condition ($\sigma > \sigma_{ys}$) invalidates the use of LEFM concepts. A research program at the INEL, funded by the U.S. Department of Energy - Basic Engineering Sciences (DOE-BES), includes testing of surface cracked specimens where failure ranges from elastic ($\sigma < \sigma_{ys}$) to elastic-plastic ($\sigma < \sigma_{uts}$). The results obtained from this research activity will be useful for predicting conditions for the crack to penetrate the wall thickness for elastic-plastic conditions and for failure for elastic and elastic-plastic conditions. No discussion of weldments has been attempted in this activity, but they are potentially the most troublesome areas from the viewpoint of a failure.

The materials accepted for fabricating tank cars consist of the following:

ASTM a515-70, Grades 55, 60, 65, and 70,

ASTM A285-70a, Grades A, B*, and C*,
ASTM A516-70a, Grades 55*, 60*, 65*, and 70*,
ASTM A537-70, Grade A*,
ASTM 302-70a, Grade B,
and AAR TC 128-70, Grades A and B.

Of these materials, those with an asterisk are included in Table 16 of ASTM A-20(Reference 7) which identifies the minimum temperature at which a minimum Charpy V-notch impact (CVN) energy has to be obtained. These requirements are not in Reference 8, but since they exist there should be substantial data available. One problem will be to estimate K_{IC} based on CVN data.

5. SUMMARY, CONCLUSIONS, AND RECOMMENDATIONS

This study was undertaken as a reconnaissance effort. It was limited in time and scope. The objectives were to attempt to define more clearly the scope of the overall problem and the areas in which future NDE and fracture mechanics/metallurgical efforts might most profitably be directed.

The investigations were guided by the accident-recovery scenario developed in Section 1 of this report, and for the NDE portions, the observable quantities discussed in Section 2. This scenario has an emphasis on the speed and safety with which valid observations can be made. It involves an increasing degree of contact with the damaged car, based on the safety information obtained in prior steps, with an increasingly detailed series of observations and an increasingly greater certainty of the status of the damaged tank car with minimum personnel exposure to hazard at each step.

The NDE and fracture mechanics work presented are very preliminary and represent a very small statistical base. Confirmatory measurements in other materials are clearly needed. Extended efforts involving measurement of additional variables are also needed. Finally, it is clear that, to be useful, these efforts must be extended to a significantly greater statistical base, with many more specimens investigated in detail.

These results were obtained with plates which had been dented in well-controlled tup-and-die tests. This process appears to leave artifacts which may or may not be typical of what would be expected in the real situation. One of these artifacts is that the observed thinning is most severe in the region where the edge of the spherical tup last contacts the plate at the outer diameter of the tup. It would be of importance to know if this type of artifact is typical in real tank car wrecks; tank-car accident photos could possibly help resolve the point.

A closer look at the utility of infrared and acoustic emission techniques is needed but is best reserved for later in any program.

5.1 Visual Observations

There are excellent statistical correlations (with, however, an admittedly small number of samples) between dent depth, dent radius, and several measures of the extent of fine surface cracking on the convex sides of dented plates. If the assumption is made that the surface cracking is indicative of thinning and at least local reduction in fracture toughness, remote measurements of denting parameters can lead to valid and at least semi-quantitative preliminary assessments, from a safe distance, of the status of a damaged tank car.

The connection between local surface cracking, thinning, and reduction in metallurgical parameters (fracture mechanics) is not yet complete. It is recommended that future efforts be made in this area.

Since the majority of the surface cracking is on the convex side of the dents, it will not be accessible for direct liquid penetrant tests in the field. If necessary, tests for surface cracking on the concealed side of the part can be performed ultrasonically; in the present instance, the liquid penetrant tests served as a rapid and accurate method for locating and quantifying areas requiring further investigation by other means.

5.2 Ultrasonic Examination

Ultrasonic techniques were used as the primary investigative tool because of the rapidity with which quantitative results can be obtained and visualized, and for other reasons summarized in Section 2.

The first ultrasonic tests were measurements of local thickness in all areas of all ten plates. These can be made rapidly and are relatively simple to automate. There was an excellent correlation between the degree of thinning, as observed ultrasonically, and measured fracture toughness parameters (Section 4). Again, the small number of samples limits the conclusions which can be made, but if this effect should prove to be general, it would become a powerful tool in rapidly obtaining detailed strength and fracture-toughness information in situ on a damaged tank car.

The ultrasonic imaging showed, as expected, that known cracks could be detected and their sizes estimated in a variety of configurations that would be likely to appear in the field. Beyond that, the detection of two classes of hidden targets which are interpreted as areas of severely reduced mechanical properties (pending further investigation) suggests that more subtle metallurgical changes of importance may be observable in the field. This also should be investigated further.

In summary, the experimental NDE effort provided very encouraging results, in nearly every instance confirming initial hypotheses on what could be expected. The results show that there are a number of field-observable NDE quantities (beyond the obvious ones of surface-breaking cracks) which seem to correlate with important mechanical parameters. In one instance a direct correlation was demonstrated; in others the correlation is inferred and should be pursued. There are reasons to believe that other important observable quantities exist.

5.3 Fracture Mechanics

The critical values of applied stress-crack size calculated for different values of K_{IC} show the usefulness of the fracture mechanics concepts and identify areas where additional work needs to be performed. Based on a fracture mechanics analysis, Section 4 identifies each of the parameters required for predicting the safety of moving a damaged tank car and provides recommendations to increase accuracy while reducing conservatism.

The data base of K_{IC} versus test temperature for A515-70 is inadequate for developing a statistically based correlation between K_{IC} and service temperatures [222 to 344 K (-60 to 160°F)]. It would be necessary to conduct an experimental test program for A515-70. An alternative approach would be to conduct a literature search for fracture toughness data for ASTM A516 Grade 70. A number of publications were found and several additional sources of A516 data identified. The availability of data would substantially reduce the extent of testing needed to develop

the desired data base. The decision of which base material and weldments would be selected should be based on relative use of the materials in fabricating (past, present, and future) railroad tank cars.

Additional recommendations are:

1. Conduct an elastic-plastic stress analysis of a typical damaged tank car. Conduct an elastic or elastic-plastic stress analysis using different loading points and techniques for moving a damaged tank car.
2. Determine the magnitude of deformation for actual damaged tank cars.
3. Establish the percent reduction in K_{IC} as a function of percent reduction in initial thickness.
4. Conduct verification tests using damaged tank cars.

6. REFERENCES

1. "Railroad Accident Report-Derailment of Louisville and Nashville Railroad Company's Train No. 584 and Subsequent Rupture of Tank Car Containing Liquid Petroleum Gas, Waverly, Tennessee, February 22, 1978," NTSB-RAR-79-1, U.S. National Transportation Safety Board, February 1979.
2. "Railroad Accident Report-Louisville and Nashville Railroad Company Freight Train Derailment and Puncture of Hazardous Materials Tank Cars, Crestview, Florida, April 18, 1979," NTSB-RAR-79-11, U.S. National Transportation Safety Board, September 1979.
3. "SPECIAL INVESTIGATION REPORT - Tank Car Structural Integrity After Derailment," NTSB-SIR-80-1, U.S. National Transportation Board, October 16, 1980.
4. R. W. Hertzberg, Deformation and Fracture Mechanics of Engineering Materials, 2nd Edition, New York, John Wiley and Sons, 1983.
5. A. S. Tetelman and A. J. McEvily, Jr., Fracture of Structural Materials, New York, John Wiley and Sons, 1967.
6. S. T. Rolfe and J. M. Barsom, Fracture and Fatigue Control in Structures, Applications of Fracture Mechanics, New Jersey, Prentice-Hall, Inc., 1977.
7. Annual Book of ASTM Standards, Part 4, 1981.
8. "Hazardous Materials Regulations of the Department of Transportation," Tariff No. BOF-6000-B, Subpart C, pp. 512-514, United States Government Printing Office, December 22, 1981.
9. A. Wilson, Lukens Steel Co., Coatesville, PA, Private Communication to M. A. Tupper, EG&G Idaho, September 15, 1983.
10. R. Brown, United States Steel, Pittsburgh, PA, Private Communication to M. A. Tupper, EG&G Idaho, September 1983.
11. C. D. Spaeder, U.S. Steel Research, Pittsburgh, PA, Private Communication to M. A. Tupper, EG&G Idaho, September 15, 1983.
12. O. W. Albritton, "Avoiding Brittle Fracture in Cold Formed ASTM A515 Steel-Metal Progress," pp. 115-120, September 1970.
13. W. W. Pellini, R. D. Eiber, and L. L. Olson, "Phase 03 Report on Fracture Properties of Tank Car Steels - Characterization and Analysis," Report No. RA-03-4-32, RPI-AAR, Tank Car Safety Research and Test Project, August 20, 1975.
14. J. C. Newman, Jr. and S. Raju, "Analysis of Surface Cracks in Finite Plates Under Tension or Bending Loads," NASA Technical Paper 1578, December 1979.

APPENDIX A

Plate Thinning Data

For each of the ten plates examined, dial micrometer measurements of the dent, ultrasonic measurements of the plate thickness, and maps of the surface cracks were made. This appendix contains the figures showing these data and the figures are as follows:

	Page Number
A-1a. Dial Micrometer Measurement of Dent Depth (DH-25-04-83-07-160)	71
A-1b. Ultrasonic Measurement of Thickness (DH-25-04-83-07-160)	71
A-1c. Map of Surface Cracks on the Convex (Bottom) Side (DH-25-04-83-07-160)	72
A-2a. Dial Micrometer Measurement of Dent Depth (DH-25-04-83-10-160)	72
A-2b. Ultrasonic Measurement of Thickness (DH-25-04-83-10-160)	73
A-2c. Map of Surface Cracks on the Convex (Bottom) Side (DH-25-04-83-10-160)	73
A-3a. Dial Micrometer Measurement of Dent Depth (DH-25-04-83-14-160)	74
A-3b. Ultrasonic Measurement of Thickness (DH-25-04-83-14-160)	74
A-3c. Map of Surface Cracks on the Convex (Bottom) Side (DH-25-04-83-14-160)	75
A-4a. Dial Micrometer Measurement of Dent Depth (DH-25-04-83-18-160)	76
A-4b. Ultrasonic Measurement of Thickness (DH-25-04-83-18-160)	76
A-4c. Map of Surface Cracks on the Convex (Bottom) Side (DH-25-04-83-18-160)	77
A-5a. Dial Micrometer Measurement of Dent Depth (DH-25-04-83-19-160)	78
A-5b. Ultrasonic Measurement of Thickness (DH-25-04-83-19-160)	78
A-5c. Map of Surface Cracks on the Convex (Bottom) Side (DH-25-04-83-19-160)	79
A-6a. Dial Micrometer Measurement of Dent Depth (DH-25-04-83-22-160)	80
A-6b. Ultrasonic Measurement of Thickness (DH-25-04-83-22-160)	80
A-6c. Map of Surface Cracks on the Convex (Bottom) Side (DH-25-04-83-22-160)	81
A-7a. Dial Micrometer Measurement of Dent Depth (DH-26-04-83-02-160)	82
A-7b. Ultrasonic Measurement of Thickness (DH-26-04-83-02-160)	82
A-7c. Map of Surface Cracks on the Convex (Bottom) Side (DH-26-04-83-02-160)	83
A-8a. Dial Micrometer Measurement of Dent Depth (DH-26-04-83-05-160)	84
A-8b. Ultrasonic Measurement of Thickness (DH-26-04-83-05-160)	84
A-8c. Map of Surface Cracks on the Convex (Bottom) Side (DH-26-04-83-05-160)	85

	Page Number
A-9a. Dial Micrometer Measurement of Dent Depth (DH-26-04-83-13-160)	86
A-9b. Ultrasonic Measurement of Thickness (DH-26-04-83-13-160)	86
A-9c. Map of Surface Cracks on the Convex (Bottom) Side (DH-26-04-83-13-160)	87
A-10a. Dial Micrometer Measurement of Dent Depth (DH-26-04-83-16-160)	87
A-10b. Ultrasonic Measurement of Thickness (DH-26-04-83-16-160)	87
A-10c. Map of Surface Cracks on the Convex (Bottom) Side (DH-26-04-83-16-160)	88

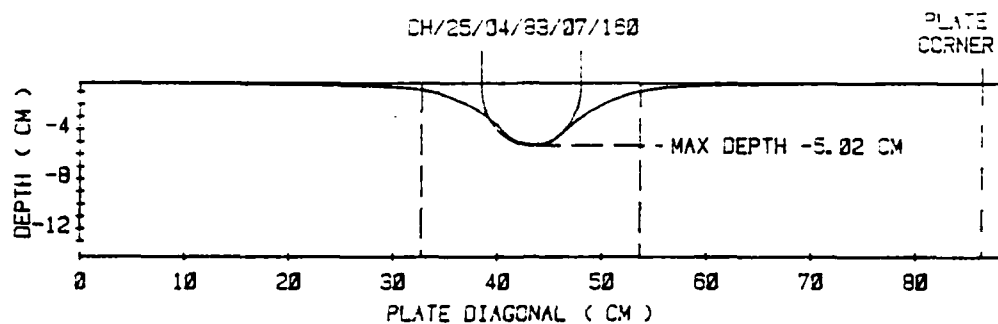


Figure A-1a. Dial Micrometer Measurement of Dent Depth (DH-25-04-83-07-160)

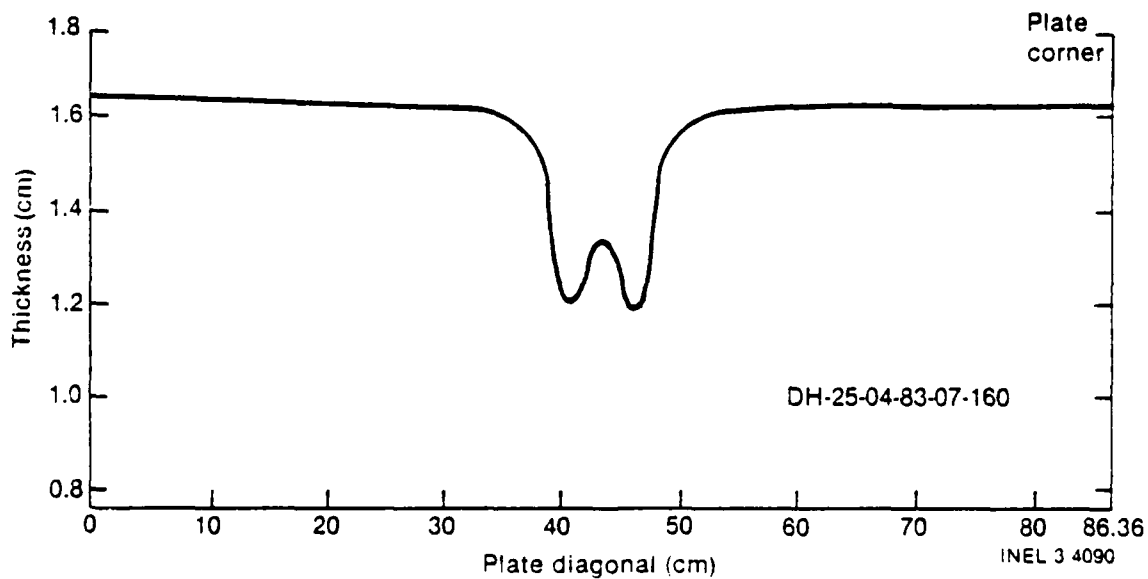


Figure A-1b. Ultrasonic Measurement of Thickness (DH-25-04-83-07-160)

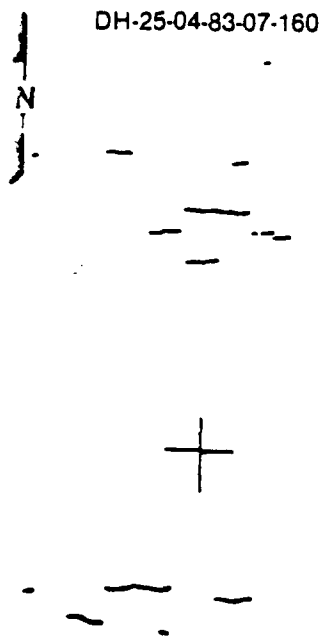


Figure A-1c. Map of Surface Cracks on the Convex (Bottom) Side
(DH-25-04-83-07-160)

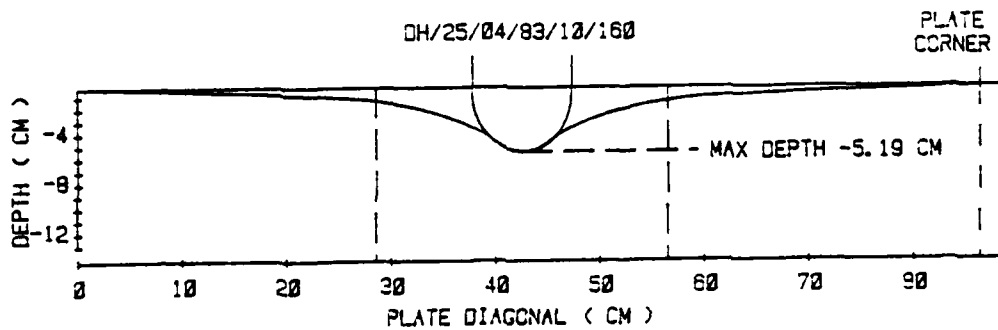


Figure A-2a. Dial Micrometer Measurement of Dent Depth (DH-25-04-83-10-160)

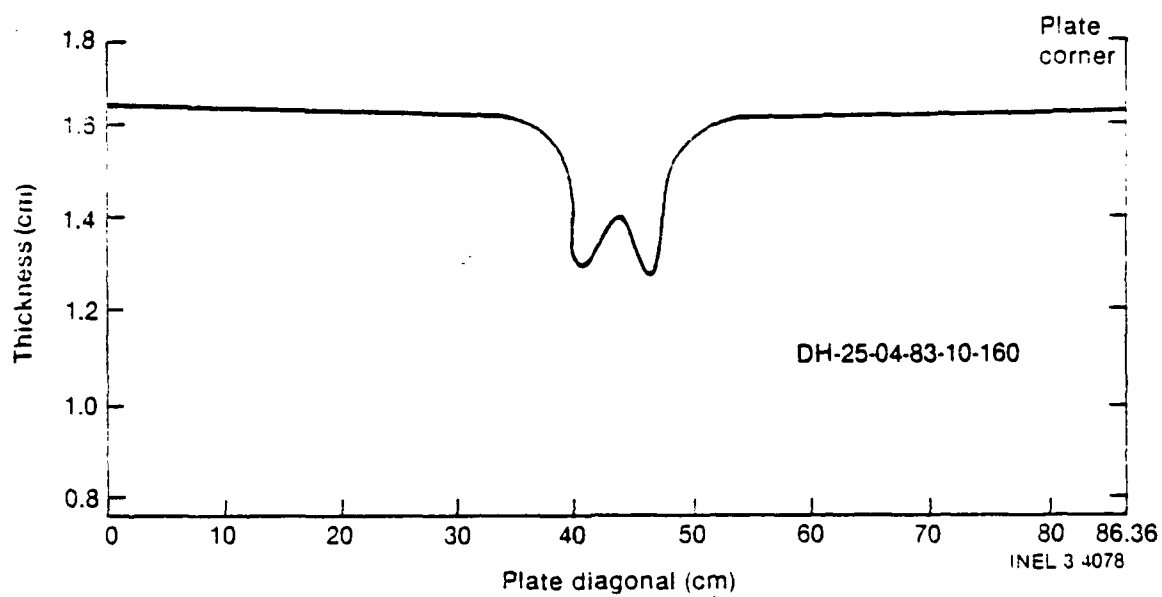


Figure A-2b. Ultrasonic Measurement of Thickness (DH-25-04-83-10-160)

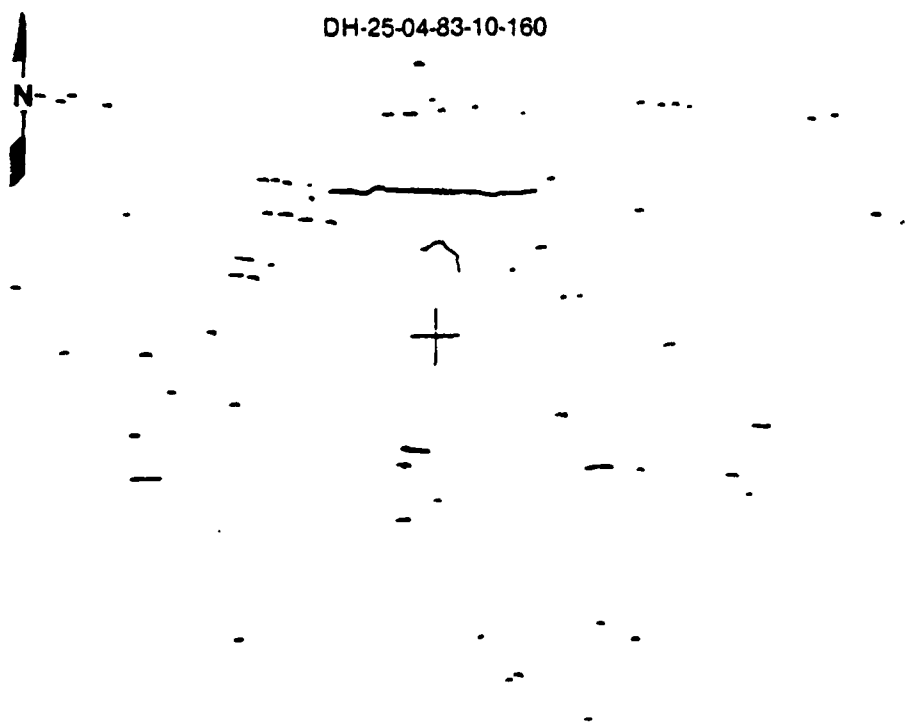


Figure A-2c. Map of Surface Cracks on the Convex (Bottom) Side (DH-25-04-83-10-160)

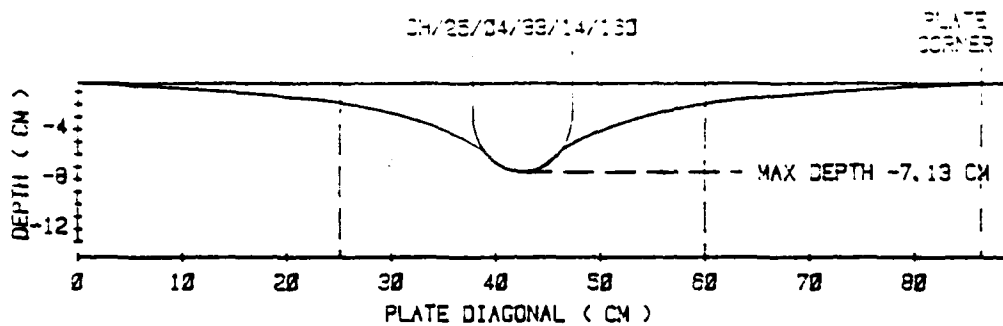


Figure A-3a. Dial Micrometer Measurement of Dent Depth (DH-25-04-83-14-160)

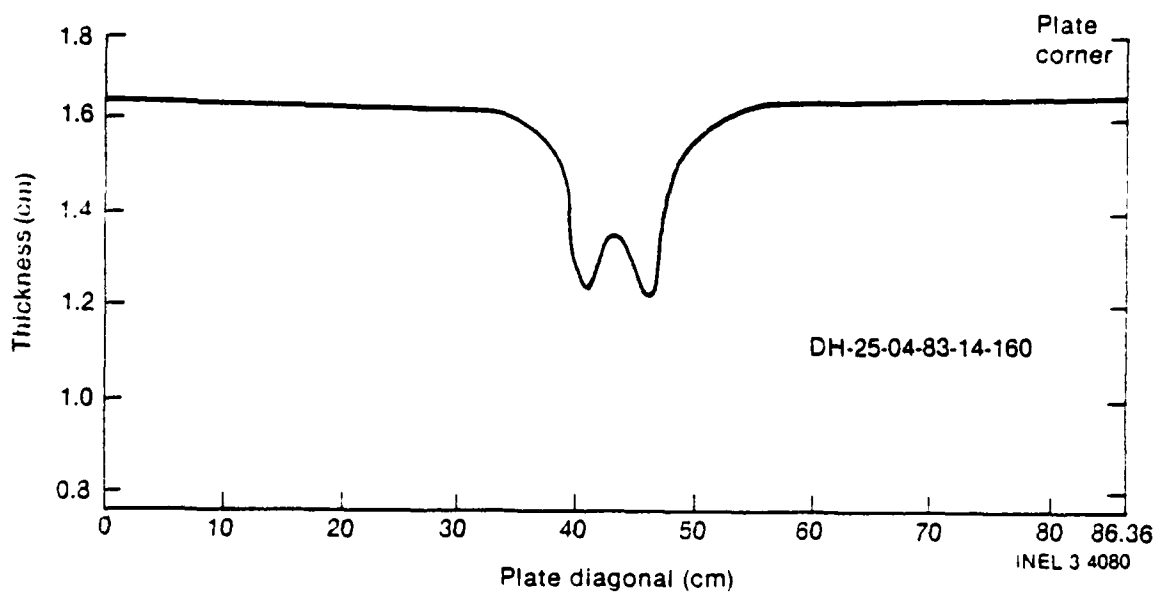


Figure A-3b. Ultrasonic Measurement of Thickness (DH-25-04-83-14-160)

DH-25-04-83-14-160



Figure A-3c. Map of Surface Cracks on the Convex (Bottom) Side
(DH-25-04-83-14-160)

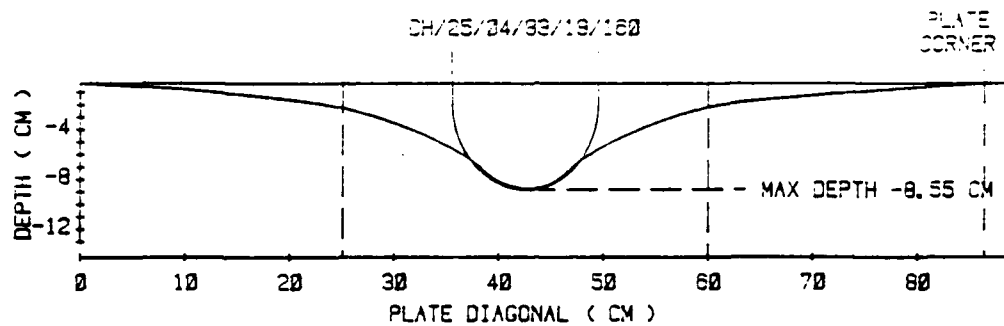


Figure A-4a. Dial Micrometer Measurement of Dent Depth (DH-25-04-83-18-160)

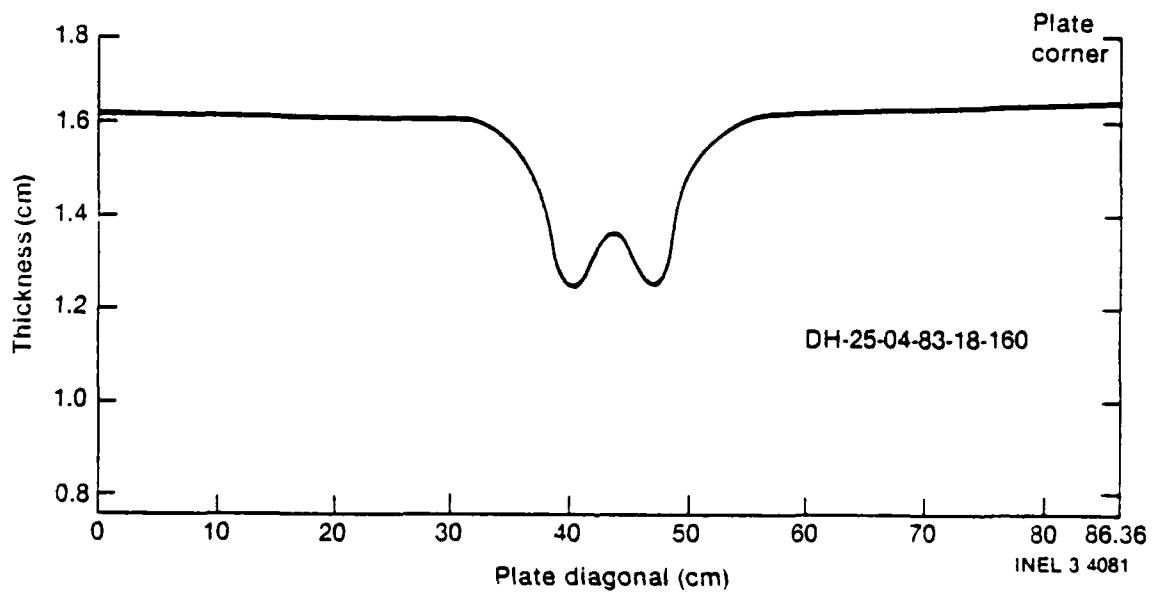


Figure A-4b. Ultrasonic Measurement of Thickness (DH-25-04-83-18-160)

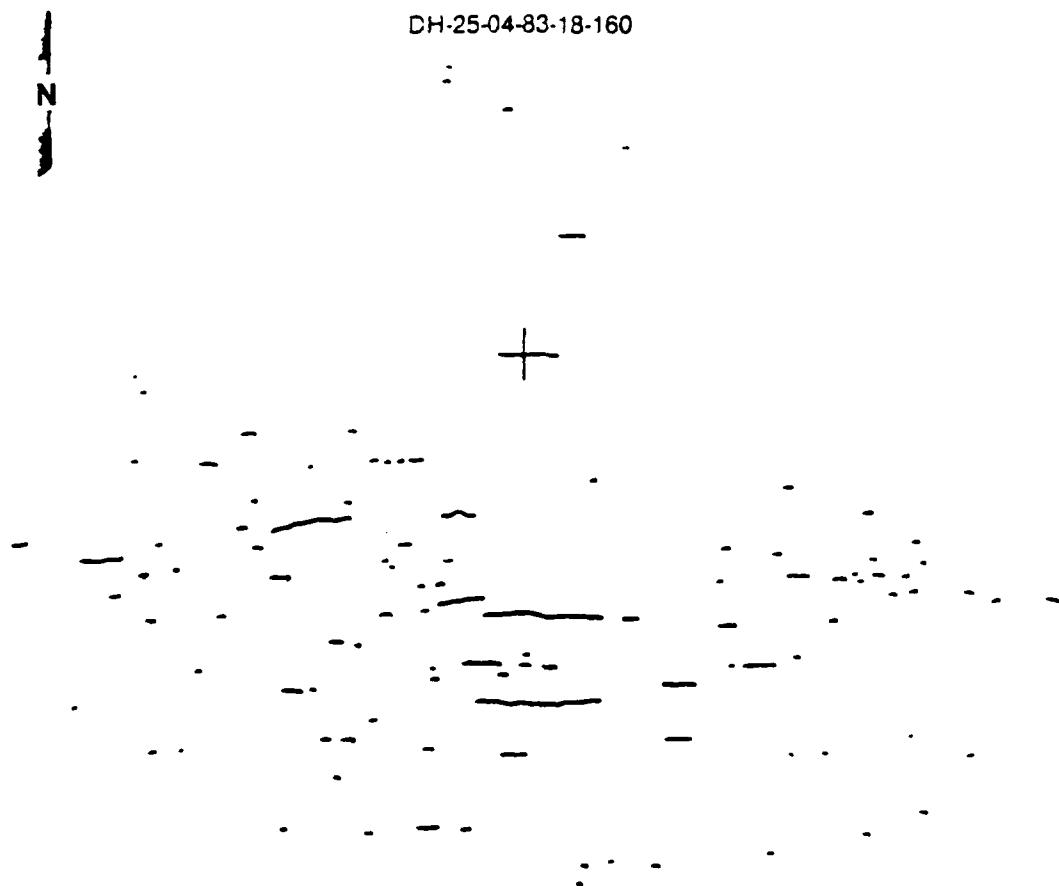


Figure A-4c. Map of Surface Cracks on the Convex (Bottom) Side
(DH-25-04-83-18-160)

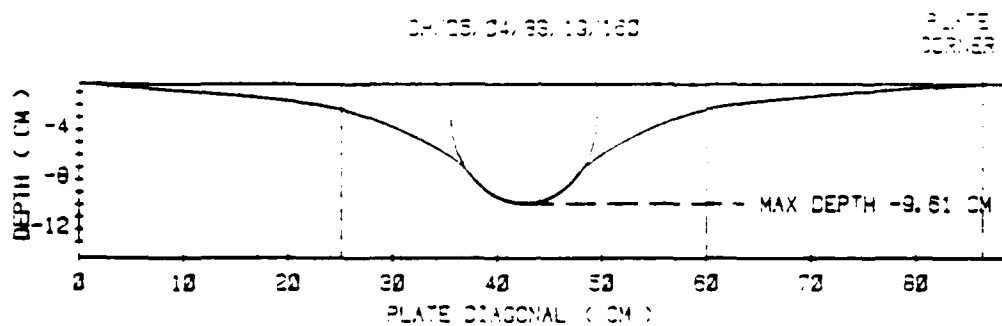


Figure A-5a. Dial Micrometer Measurement of Dent Depth (DH-25-04-83-19-160)

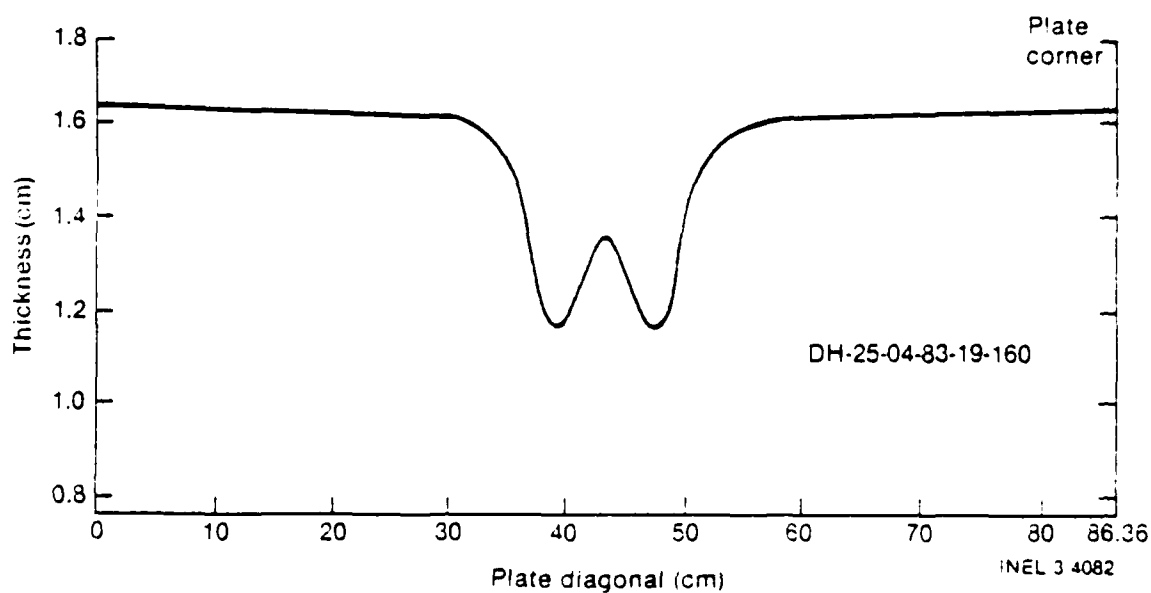


Figure A-5b. Ultrasonic Measurement of Thickness (DH-25-04-83-19-160)

DH-25-04-83-19-160

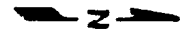


Figure A-5c. Map of Surface Cracks on the Convex (Bottom) Side
(DH-25-04-83-19-160)

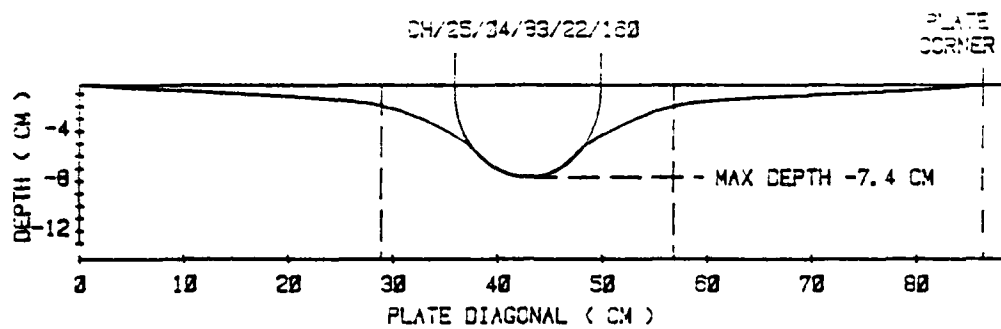


Figure A-6a. Dial Micrometer Measurement of Dent Depth (DH-25-04-83-22-160)

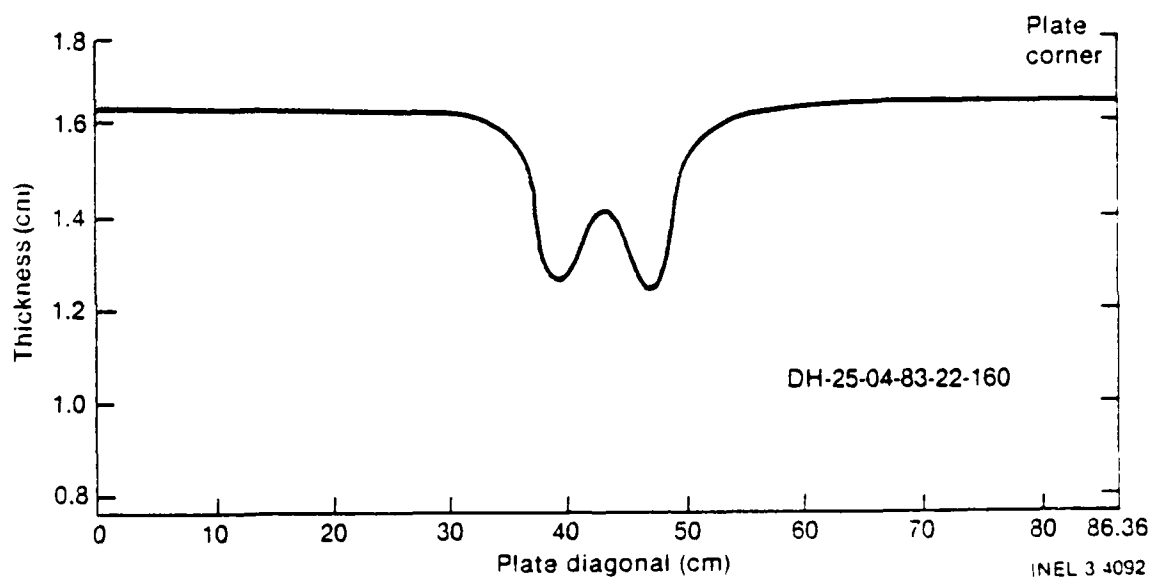


Figure A-6b. Ultrasonic Measurement of Thickness (DH-25-04-83-22-160)

DH-25-04-83-22-160

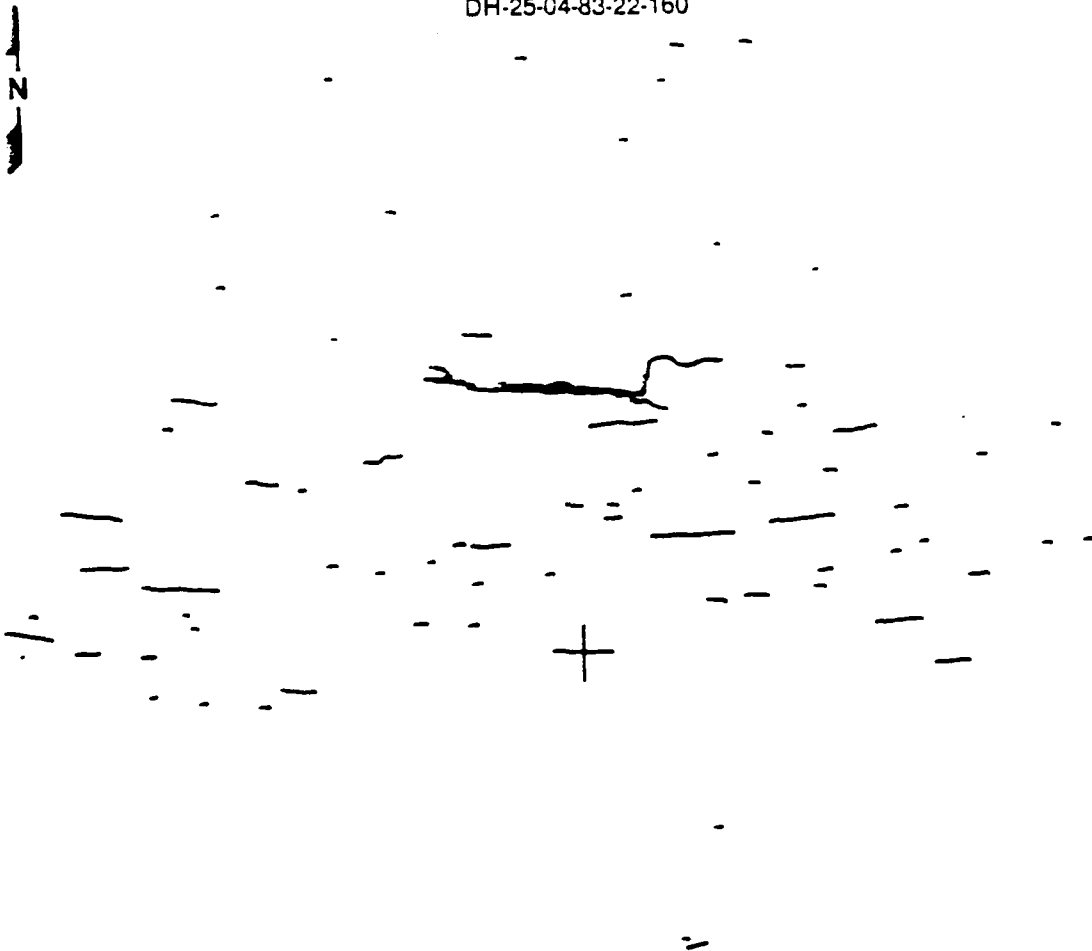


Figure A-6c. Map of Surface Cracks on the Convex (Bottom) Side
(DH-25-04-83-22-160)

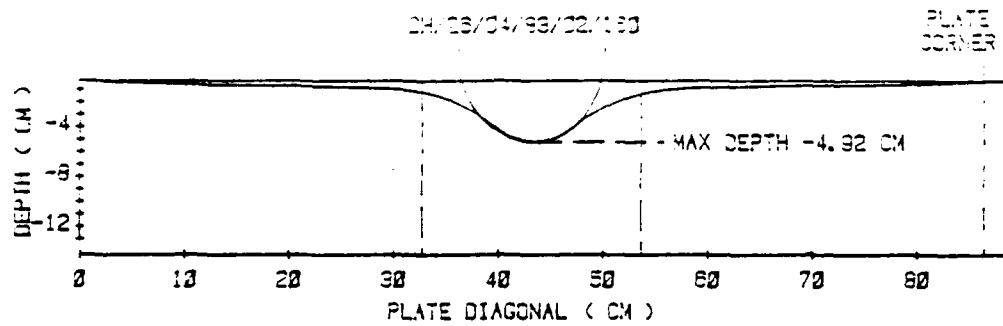


Figure A-7a. Dial Micrometer Measurement of Dent Depth (DH-26-04-83-02-160)

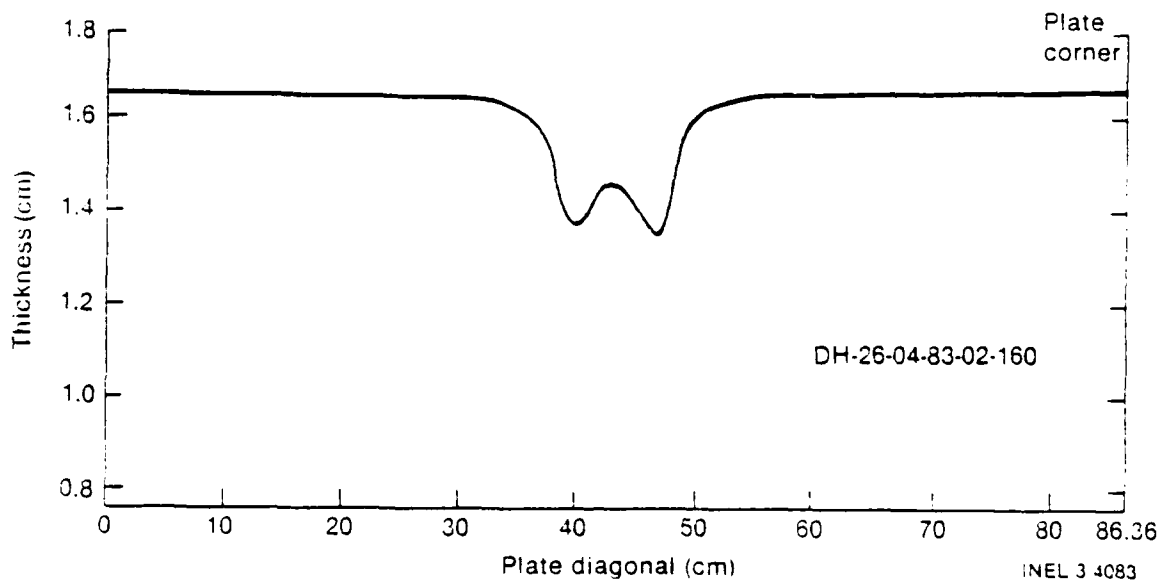


Figure A-7b. Ultrasonic Measurement of Thickness (DH-26-04-83-02-160)

DH-26-04-83-02-160

N



Figure A-7c. Map of Surface Cracks on the Convex (Bottom) Side
(DH-26-04-83-02-160)

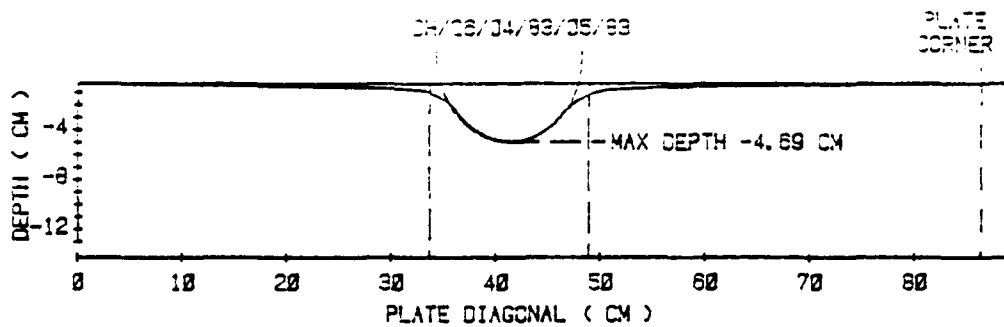


Figure A-8a. Dial Micrometer Measurement of Dent Depth (DH-26-04-83-05-160)

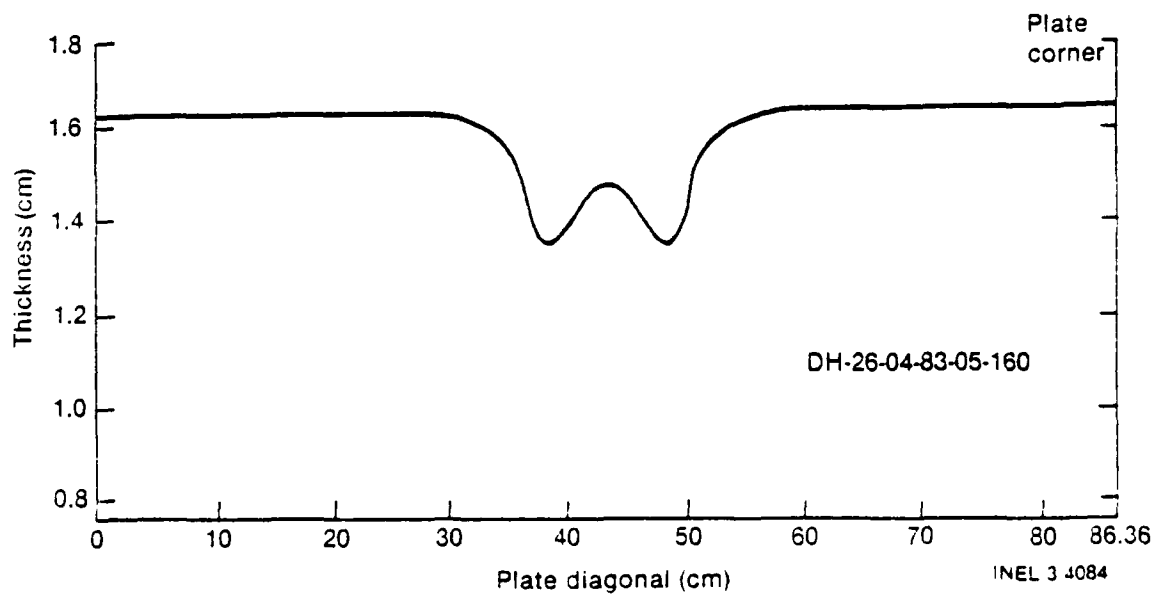


Figure A-8b. Ultrasonic Measurement of Thickness (DH-26-04-83-05-160)

N

DH-26-04-83-05-160



Figure A-8c. Map of Surface Cracks on the Convex (Bottom) Side
(DH-26-04-83-05-160)

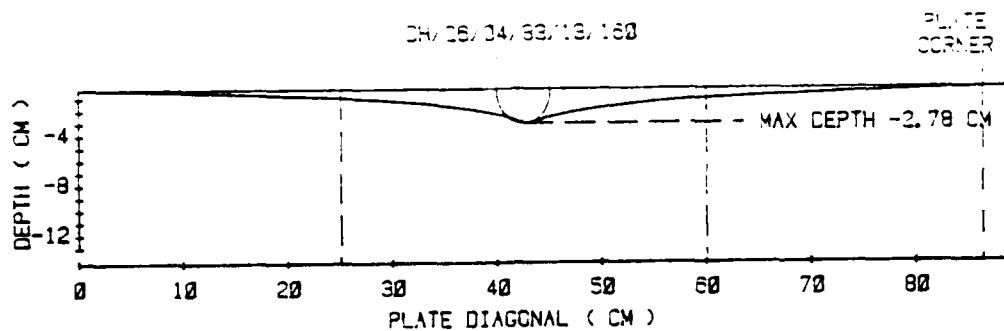


Figure A-9a. Dial Micrometer Measurement of Dent Depth (DH-26-04-83-13-160)

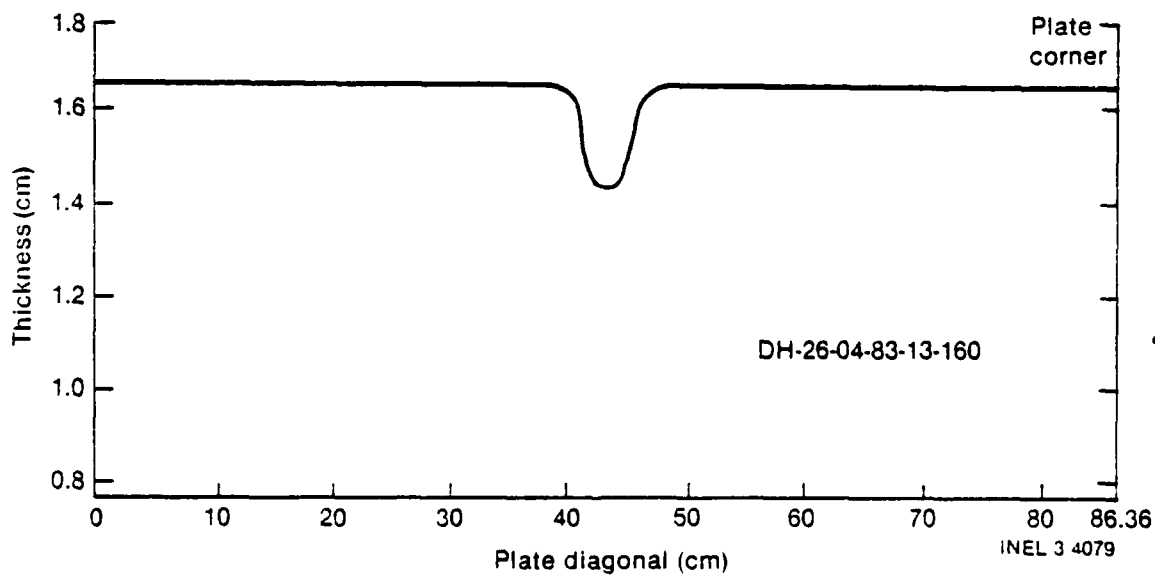


Figure A-9b. Ultrasonic Measurement of Thickness (DH-26-04-83-13-160)

DH-26-04-83-13-160

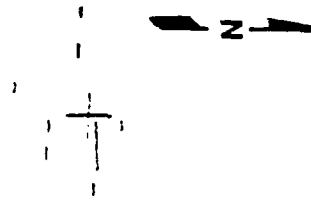


Figure A-9c. Map of Surface Cracks on the Convex (Bottom) Side
(DH-26-04-83-13-160)

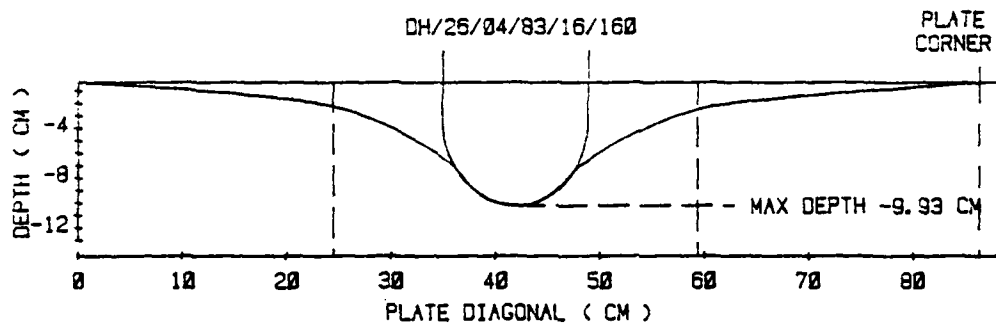


Figure A-10a. Dial Micrometer Measurement of Dent Depth (DH-26-04-83-16-160)

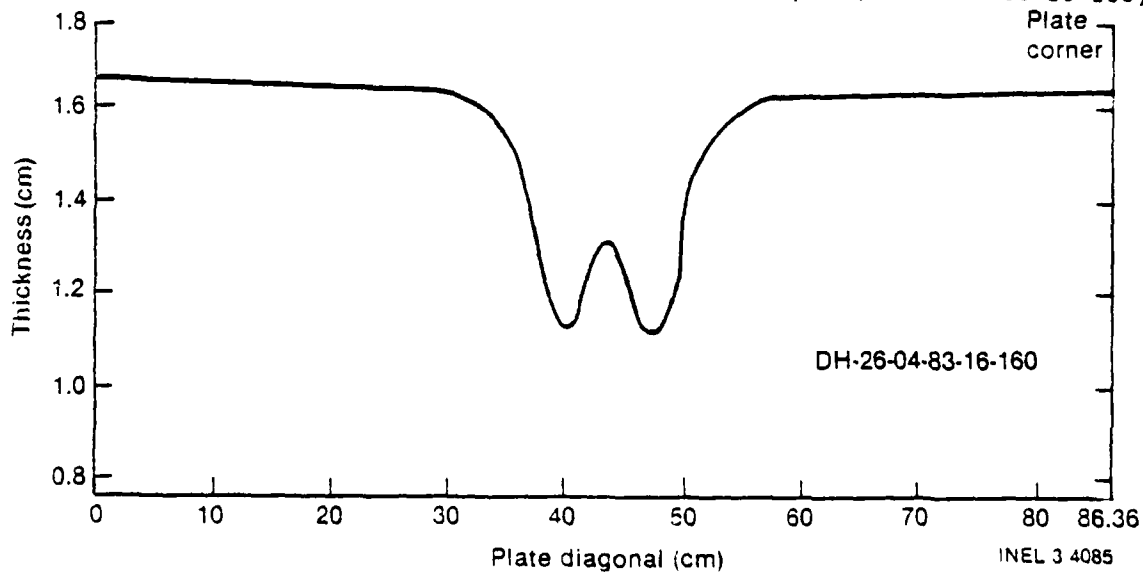


Figure A-10b. Ultrasonic Measurement of Thickness (DH-26-04-83-16-160)

DH-26-04-83-16-160

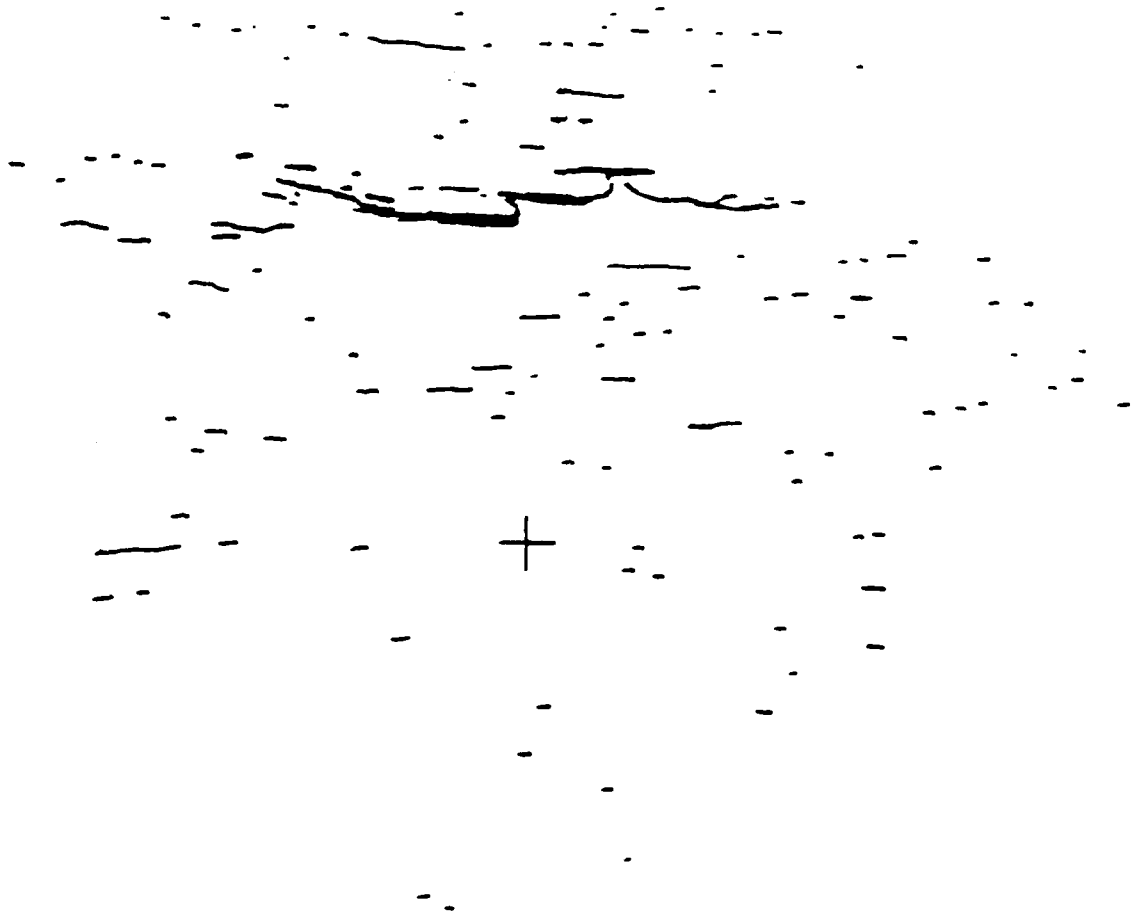


Figure A-10c. Map of Surface Cracks on the Convex (Bottom) Side
(DH-26-04-83-16-160)

LIST OF SYMBOLS

LEFM	Linear-elastic fracture mechanics
K_I	Applied stress intensity factor
K_{Ic}	Plane strain fracture toughness
σ	Applied stress
Y	A geometric parameter
CVN	Charpy V-notch impact energy
NDTT	Nil-ductility transition temperature
MPa	Mega pascal
ksi	Kilo pounds per square inch
M	Stress-intensity boundary correction factor
a	Crack depth
Q	$1 + 1.464 (a/c)^{1.65}$ (shape factor for elliptical crack)
M	$[M_1 + M_2 (a/t)^2 + M_3 (a/t)^4] f_\phi f_w g$
M_1	$1.13 - 0.09 (a/c)$
M_2	$-0.54 + \frac{0.89}{0.2 + a/c}$
M_3	$0.5 - \frac{1.0}{0.65 + a/c} + 14 (1.0 - a/c)^{24}$

g	$1 + [0.1 + 0.35(a/t)^2] (1 - \sin \phi)^2$ [where ϕ is measured around the circumference of the flaw starting at $\phi = 0$ (free surface) to $\phi = 90^\circ$ (maximum depth)]
$f_\phi =$	$[(a/c)^2 \cos^2 \phi + \sin^2 \phi]^{1/4}$
$f_w =$	Finite width correction = $[\sec \frac{\pi c}{2b} \sqrt{(a/t)}]^{1/2}$
c	One-half crack length
t	Material thickness
$a/2c$	Aspect ratio
m	Meter
mm	Millimeter
$in.$	Inches
$K_{critical}$	Critical stress intensity factor
$\sigma_{critical}$	Critical stress
σ_{uts}	Ultimate tensile strength
σ_{ys}	Yield stress
σ_{app}	Applied stress
MHz	Megahertz

DISTRIBUTION LIST

<u>No. of Copies</u>	<u>Organization</u>	<u>No. of Copies</u>	<u>Organization</u>
12	Commander Defense Technical Info Center ATTN: DTIC-DDA Cameron Station Alexandria, VA 22314	1	Commander US Army Communications Rsch and Development Command ATTN: AMSEL-ATDD Fort Monmouth, NJ 07703
1	Commander US Army Materiel Command ATTN: AMCDRA-ST 5001 Eisenhower Avenue Alexandria, VA 22333	1	Commander US Army Electronics Research and Development Command Technical Support Activity ATTN: AMDSD-L Fort Monmouth, NJ 07703
1	Commander Armament R&D Center US Army AMCCOM ATTN: SMCAR-TDC Dover, NJ 07801	1	Commander US Army Missile Command ATTN: AMSMI-R Redstone Arsenal, AL 35898
1	Commander Armament R&D Center US Army AMCCOM ATTN: SMCAR-TSS Dover, NJ 07801	1	Commander US Army Missile Command ATTN: AMSMI-YDL Redstone Arsenal, AL 35898
1	Commander US Army Armament, Munitions & Chemical Command ATTN: AMSMC-LEP-L, Tech Lib Rock Island, IL 61299	1	Commander US Army Tank Automotive Command ATTN: AMSTA-TSL Warren, MI 48090
1	Director Benet Weapons Laboratory Armament R&D Center US Army AMCCOM ATTN: SMCAR-LCB-TL Watervliet, NY 12189	1	Director US Army TRADOC Systems Analysis Activity ATTN: ATAA-SL, Tech Lib White Sands Missile Range NM 88002
1	Commander US Army Aviation Research and Development Command ATTN: AMSAV-E 4300 Goodfellow Blvd St. Louis, MO 63120	1	Director US Army Air Mobility Research and Development Laboratory Ames Research Center Moffett Field, CA 94035

DISTRIBUTION LIST

<u>No. Of Copies</u>	<u>Organization</u>	<u>Aberdeen Proving Ground</u>
10	Department of Transportation Federal Railroad Administration ATTN: Ms Claire Orth (COTR) Room 5423 400 Seventh Street, S.W., Washington, DC 20590	Dir, USAMSAA ATTN: AMXSY-D AMXSY-MP, H. Conen Cdr, USATECOM ATTN: AMSTE-TO-F Cdr, CRDC, AMCCOM ATTN: SMCCR-RSP-A SMCCR-MU SMCCR-SPS-IL
5	Idaho National Engineering Laboratory EG&G Idaho, Inc. ATTN: Mr. Ken G. Koller Post Office Box 1625 Idaho Falls, ID 83415	
1	HQDA DAMA-ART-M Washington, DC 20310	
1	Commandant US Army Infantry School ATTN: ATSH-CD-CSO-OR Fort Benning, GA 31905	
1	Commander US Army Development & Employment Agency ATTN: MODE-TED-SAB Fort Lewis, WA 98433	
1	AFWL/SUL Kirtland AFB, NM 87117	

USER EVALUATION SHEET/CHANGE OF ADDRESS

This Laboratory undertakes a continuing effort to improve the quality of the reports it publishes. Your comments/answers to the items/questions below will aid us in our efforts.

1. BRI Report Number _____ Date of Report _____
2. Date Report Received _____
3. Does this report satisfy a need? (Comment on purpose, related project, or other area of interest for which the report will be used.) _____

4. How specifically, is the report being used? (Information source, design data, procedure, source of ideas, etc.) _____

5. Has the information in this report led to any quantitative savings as far as man-hours or dollars saved, operating costs avoided or efficiencies achieved etc? If so, please elaborate. _____

6. General Comments. What do you think should be changed to improve future reports? (Indicate changes to organization, technical content, format, etc.) _____

Name _____
Organization _____
CURRENT ADDRESS Address _____
City, State, Zip _____

7. If indicating a Change of Address or Address Correction, please provide the New or Correct Address in Block 6 above and the Old or Incorrect address below.

Name _____
Organization _____
OLD ADDRESS Address _____
City, State, Zip _____

(Remove this sheet along the perforation, fold as indicated, staple or tape closed, and mail.)

----- FOLD HERE -----

Director
US Army Ballistic Research Laboratory
ATTN: AMXBR-OD-ST
Aberdeen Proving Ground, MD 21005-5066

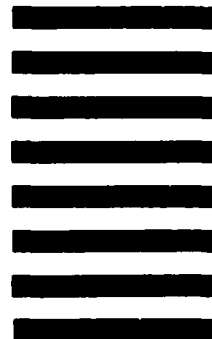


NO POSTAGE
NECESSARY
IF MAILED
IN THE
UNITED STATES

OFFICIAL BUSINESS
PENALTY FOR PRIVATE USE, \$300

BUSINESS REPLY MAIL
FIRST CLASS PERMIT NO 12062 WASHINGTON, DC
POSTAGE WILL BE PAID BY DEPARTMENT OF THE ARMY

Director
US Army Ballistic Research Laboratory
ATTN: AMXBR-OD-ST
Aberdeen Proving Ground, MD 21005-9989



----- FOLD HERE -----

END

FILMED

3-85

DTIC